Direct Torque Control of a Permanent Magnet synchronous Motor

D A V I D O C E N

KTH Signals
Sensors and Systems

Master's Degree Project
Stockholm, Sweden 2005

IR-RT-EX-0509

Abstract

This work presents an improved variant of the Direct Torque Control (DTC) for a Permanent Magnet Synchronous Motor (PMSM). The improved DTC use a higher number of voltage space vectors by introducing a kind of Space Vector Modulation technique. The higher number of space vectors are tabulated in more precise switch tables which also take the emf induced in the stator windings into account. The emf voltage significantly affect the motor behavior from a given space vector. It is discussed how the switch tables are constructed. Experiments from the classical and improved DTC are compared and show that the torque, flux linkage and stator current ripples are significantly decreased with the improved DTC.

Acknowledgment

I have worked on this thesis at the Universitat Politècnica de Catalunya in Terrassa in the Motion Control and Industrial Applications Group from October 2004 until March 2005. I would like to say thanks to my supervisor in Barcelona, Dr. Luis Romeral and other people in the UPC who helped me during this work. Also I would like to thank Karl Henrik Johansson at S3, KTH.

Stockholm, May 2005
David Ocen

Contents

Notations

δ	load angle
i_d	d-axis current
i_q	q-axis current
i_s	current vector value, $\left\|\boldsymbol{i}_{qd}\right\|$
$\boldsymbol{K}_s$	Park Transform
λ_d	d-axis flux
λ_q	q-axis flux
λ_s	flux vector value, $\left\|\boldsymbol{\Lambda}_{qd}\right\|$
L_d	d-axis inductance
L_q	q-axis inductance
L_M	q and d-axis inductance, used when $L_q = L_d = L_M$
$\boldsymbol{L}_s$	stator windings self and mutual inductance matrix
θ_m	rotor position, mechanical angle
θ_r	rotor position, electrical angle
ω_m	angular velocity, mechanical angle
ω_r	angular velocity, electrical angle
P	number of magnetic poles, two for each magnet
$\Re$	magnetic reluctance
$\boldsymbol{R}_s$, r_s	stator winding resistance
$\boldsymbol{v}_{abc}$	stator winding voltage vector
v_d	d-axis voltage
v_q	q-axis voltage
v_s	emf/speed-voltage, $\omega_r\lambda_s$

CSI	Current Source Inverter
DTC	Direct Torque Control
FOC	Field Oriented Control
SVM	Space Vector Modulation
VSI	Voltage Source Inverter
PMSM	Permanent Magnet Synchronous Motor

I. Introduction

Direct Torque Control was introduced in the 1980´s for Induction Motors as a new approach for torque and flux control. Direct Torque Control (DTC) directly controls the inverter states based on the errors between the reference and estimated values of torque and flux. It selects one of six voltage vectors generated by a Voltage Source Inverter to keep torque and flux within the limits of two hysteresis bands.
Characteristics of DTC are:

- good dynamic torque response
- robustness
- low complexity

The main drawback of the DTC is its relatively high torque and flux ripple.
In this work a background is presented in chapter 1 and 2. Chapter 1 derives the motor model equations used for simulations with Simulink. Chapter 2 presents some common control techniques used for control of Permanent Magnet Synchronous Motors (PMSM). The classical DTC scheme is presented and analyzed in chapter 3. In chapter 4 one of the improved DTC schemes proposed in the research literature is presented and compared with the classical. The improved scheme is called Discrete Space Vector Modulation (DSVM) – DTC, and address the problem with torque ripple in the basic DTC system.
In chapter 5 simulation and experimental results are presented and compared. Both systems are modeled in Simulink and then tested on a dSPACE platform for the experimental results.

Chapter 1 Permanent Magnet Synchronous Motor

In this chapter the motor model used for simulations is derived. The model focuses on the fundamental frequency component. The magnetic circuits are assumed linear, stator windings are considered sinusoidally distributed and the magnetic fields are assumed equal along the rotor axis, so no end fringing effects are taken into account.
The model can be found in [4,8], but is also found in most papers and books treating the PM synchronous motor.

1.1 Derivation of motor equations, abc-frame

The Permanent Magnet Synchronous Motor is a three-phase AC machine. The windings are Y-connected and displaced 120 electrical degrees in space.

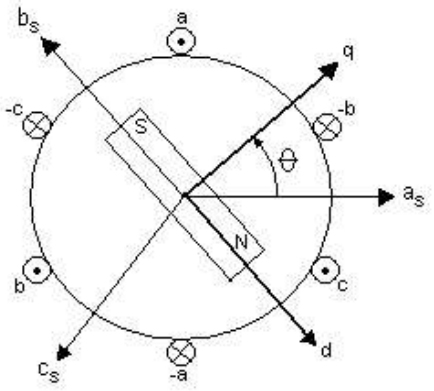

Figure 1.1, A simplified sketch of a PM motor showing stator windings, rotor magnet and their magnetic axes

The stator windings consists of individual coils connected and wound in different slots so as to approximate a sinusoidal distribution, to minimize the space harmonics [5]. In Figure 1.1 the stator windings are depicted as single coils together with their resultant magnetic axes.

The material of which the rotor and stator are made of has a lower reluctance than the air-gap between them, and therefore almost all the magnetic fields are concentrated to the air-gap. Hence, one can ignore the magnetic reluctance in the stator and rotor and assume all magnetic energy is in the air-gap. Also, because the air-gap is short in comparison to the radius of the rotor, one can assume the fields are constant across the air-gap. The fields are supposed radially directed because they tend to choose the lowest reluctance path.

Figure 1.2 shows the magnetic field of a concentrated winding.

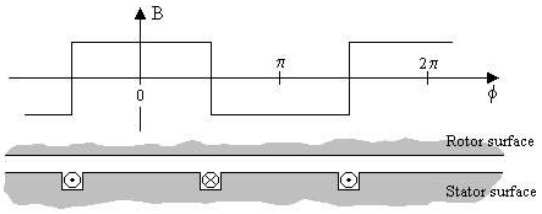

Figure 1.2, B-field of a concentrated winding that spans π radians

When a stator winding is distributed over several slots the resultant field more resembles a sine wave. Figure 1.3 shows a distributed winding and the fundamental component of the magnetic field.

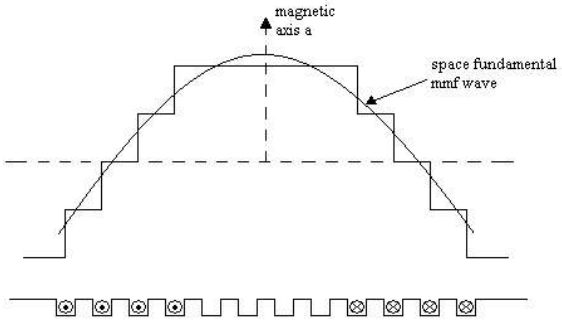

Figure 1.3, Magnetic field of a distributed winding
and its fundamental frequency component

Magneto Motive Force

Consider the integral $mmf = \int \boldsymbol{H} \cdot \boldsymbol{dl}$ [A], where the integral path is across one air-gap. If we evaluate $V_m = \oint \boldsymbol{H} \cdot \boldsymbol{dl}$ along the integral path shown in figure 1.4 and keep in mind that the magnetic field was confined to the air-gap gives, $V_m = 2\int \boldsymbol{H} \cdot \boldsymbol{dl}$, since both air-gaps contribute equally to the integral.

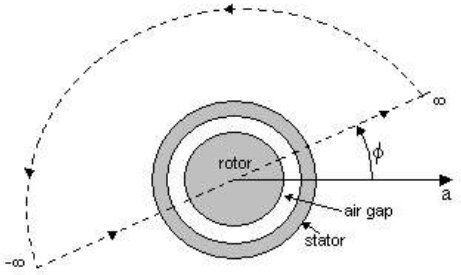

Figure 1.4, Integral path for $V_m = \oint \boldsymbol{H} \cdot \boldsymbol{dl}$

If the winding is sinusoidally distributed then $V_m = NI\cos(\varphi)$, so that $mmf = NI/2\cos(\varphi)$.

φ is measured from winding *a*'s magnetic axis.
Mmf for windings *b* and *c* are similar, the difference is a space-phase delay by 2π/3 and 4π/3 radians respectively,

$$mmf_a = \frac{N I}{2}\cos(\varphi) \tag{1.1}$$

$$mmf_b = \frac{N I}{2}\cos(\varphi - 2\pi/3) \tag{1.2}$$

$$mmf_c = \frac{N I}{2}\cos(\varphi + 2\pi/3) \tag{1.3}$$

Rotating mmf wave

When the three stator windings are displaced in space by 2π/3 electrical radians and fed by a balanced set of sinusoidal voltages the result is a single rotating mmf wave with the same frequency and with amplitude 3/2 times that of each winding.
For phase *a* the time dependent mmf wave can be written

$$F_a = F_{max}\cos(\theta)\cos(\omega t) \quad , \tag{1.4}$$

where θ is measured from *a*'s magnetic axis.
Using the equality

$$\cos(a)\cos(b) = \frac{1}{2}\cos(a-b) + \frac{1}{2}\cos(a+b) \quad , \tag{1.5}$$

one may rewrite F_a as

$$F_a = F_{max}\left(\frac{1}{2}\cos(\theta - \omega t) + \frac{1}{2}\cos(\theta + \omega t)\right) \quad . \tag{1.6}$$

This is the superposition of two rotating waves; $F_a^+ = \frac{1}{2} F_{max} \cos(\theta - \omega t)$ in the positive or counterclockwise direction and $F_a^- = \frac{1}{2} F_{max} \cos(\theta + \omega t)$ in the negative direction.
Windings *b* and *c* are phase delayed 2π/3 and 4π/3 respectively both in space and time phase which results in the following expressions,

$$F_b = F_b^+ + F_b^- = F_{max}\left(\frac{1}{2}\cos(\theta - \omega t) + \frac{1}{2}\cos(\theta + \omega t + 2\pi/3)\right) \tag{1.7}$$

$$F_c = F_c^+ + F_c^- = F_{max}\left(\frac{1}{2}\cos(\theta - \omega t) + \frac{1}{2}\cos(\theta + \omega t - 2\pi/3)\right) \quad . \tag{1.8}$$

Summing the positive and negative mmf waves individually gives

$$F_a^+ + F_b^+ + F_c^+ = \frac{3}{2} F_{max} \cos(\theta - \omega t) \tag{1.9}$$

and

$$F_a^- + F_b^- + F_c^- = 0 \quad . \tag{1.10}$$

Hence the resultant wave, F, is

$$F = \frac{3}{2} F_{max} \cos(\theta - \omega t) \quad . \tag{1.11}$$

PMSM motor equations

In a motor with more than one magnet the electrical angular velocity differ from the mechanical. Their relationship is

$$\theta_r = \frac{P}{2} \theta_m \quad , \tag{1.12}$$

where θ_r is the rotor position measured in electrical degrees, θ_m in mechanical degrees and P is the number of poles (two for each magnet).

The voltage, v, over each stator winding is the sum of the resistive voltage drop, ri, and the voltage induced from the time varying flux linkage, $d\lambda/dt$,

$$\begin{aligned} v_a &= r_a i_a + \frac{d}{dt} \lambda_a \\ v_b &= r_b i_b + \frac{d}{dt} \lambda_b \\ v_c &= r_c i_c + \frac{d}{dt} \lambda_c \quad . \end{aligned} \tag{1.13}$$

The stator windings are wound with the same number of turns so the resistance is equal in all three windings, $r_a = r_b = r_c = r_s$.
In matrix form these voltage equations (1.13) becomes,

$$\boldsymbol{V}_{abc} = \boldsymbol{R}_s \boldsymbol{i}_{abc} + \frac{d}{dt} \boldsymbol{\Lambda}_{abc} = \begin{bmatrix} r_s & 0 & 0 \\ 0 & r_s & 0 \\ 0 & 0 & r_s \end{bmatrix} \begin{bmatrix} i_a \\ i_b \\ i_c \end{bmatrix} + \frac{d}{dt} \begin{bmatrix} \lambda_a \\ \lambda_b \\ \lambda_c \end{bmatrix} \tag{1.14}$$

Flux linkage in a linear magnetic circuit is the product of inductance and current. The motor model was assumed linear, which is a fairly accurate approximation if saturation

does not occur.
Hence,

$$\boldsymbol{\Lambda}_{abc} = \boldsymbol{L}_s \boldsymbol{i}_{abc} + \boldsymbol{\lambda}_m \quad , \tag{1.15}$$

where $\boldsymbol{L}_s$ contains self and mutual inductances and $\boldsymbol{\lambda}_m$ is the flux through the stator windings due to the permanent magnet.

Inductance matrix $\boldsymbol{L}_s$

$$\boldsymbol{L}_s = \begin{bmatrix} L_{aa} & L_{ab} & L_{ac} \\ L_{ab} & L_{bb} & L_{bc} \\ L_{ac} & L_{bc} & L_{cc} \end{bmatrix} \tag{1.16}$$

The diagonal elements in the inductance matrix $\boldsymbol{L}_s$ are self inductances and the off diagonal elements are mutual inductances. The matrix is symmetric because the flux coupling between two windings is equal in both directions.
A current in a stator winding gives rise to a leakage flux and a magnetizing flux. The magnetizing flux is confined to the air-gap and give rise to the rotating mmf wave. Leakage flux is assumed to only affect its own winding. In a magnetically linear circuit self inductance is the ratio of the flux flowing through the winding to the current flowing in the winding with all other currents set to zero.
Let the self inductance be $L_{aa} = L_{ls} + L_m$, where L_{ls} is the leakage inductance and L_m the magnetizing inductance.
Now the magnetizing inductance is generally not constant; reluctance may depend on rotor position. For example the, unrealistic, rotor depicted in Figure 1.1 would have had a lower reluctance path along its d-axis because iron has lower reluctance than air.
This phenomenon is called *saliency* and is present in some permanent magnet motors, especially those with a high number of pole pairs.

Let $L_{aa} = L_{ls} + L_{mq}$ when the rotor quadrature axis is parallel with magnetic axis *a*, and $L_{aa} = L_{ls} + L_{md}$ when the direct axis is.

The magnetic field from the rotor magnet has a preferred direction along the direct axis. Reluctance is therefore lower along the d-axis, $\Re_d < \Re_q$. An inductance may be expressed as $L = N^2/\Re$, which implies that

$$L_{mq} < L_{md} \quad . \tag{1.17}$$

Thus,

$$L_{ls} + L_{mq} \leq L_{aa} \leq L_{ls} + L_{md} \tag{1.18}$$

L_{aa} varies periodically with twice the speed of the rotor since when the rotor has rotated π radians the same magnetic characteristics are restored. (It is only the varying reluctance path which is considered here, the PM flux is considered later).
The min values of L_{aa} occurs at

$$\theta_r = 0, \pi, 2\pi, ...$$

and maximum values at

$$\theta_r = \frac{\pi}{2}, \frac{3\pi}{2}, ...$$

Assume $L_{aa}(\theta_r)$ varies sinusoidally, then

$$L_{aa} = L_{ls} + L - L_{\Delta}\cos(2\theta_r) \quad , \tag{1.19}$$

where L is the average value of the magnetizing inductance and L_{Δ} half the amplitude of the sinusoidal varying magnetizing inductance.

The L_{bb} and L_{cc} self inductances can be found from eq. (1.19) by introducing a 2π/3 and 4π/3 radians space-phase lag respectively

$$L_{bb} = L_{ls} + L - L_{\Delta}\cos\left(2(\theta_r - 2\pi/3)\right) = L_{ls} + L - L_{\Delta}\cos(2\theta_r + 2\pi/3) \tag{1.20}$$

$$L_{cc} = L_{ls} + L - L_{\Delta}\cos\left(2(\theta_r - 4\pi/3)\right) = L_{ls} + L - L_{\Delta}\cos(2\theta_r - 2\pi/3) \tag{1.21}$$

Mutual inductance

Assume the mutual inductance is only due to the space mmf wave. Inductance was assumed to vary sinusoidally around a constant value,

$$L_{aa} = L_{ls} + L - L_{\Delta}\cos(2\theta_r) \quad . \tag{1.22}$$

Since an inductance may be expressed as $L = N^2/\Re$, the reluctance for L_{aa} (without the leakage inductance) may be written

$$\Re^{-1} = \alpha_1 - \alpha_2\cos(2\theta_r) \tag{1.23}$$

or by making use of $\Re = l/(\mu A)$ the equivalent air-gap length is

$$l^{-1}(\theta_r) = \beta_1 - \beta_2\cos(2\theta_r) \quad . \tag{1.24}$$

When measured an angle φ from a's magnetic axis

$$l^{-1}(\varphi-\theta_r)=\beta_1-\beta_2\cos(2\varphi-2\theta_r) \quad . \tag{1.25}$$

The flux density with all currents set to zero except i_a is

$$B_r=\mu\, mmf_a(\varphi)l^{-1}(\varphi-\theta_r)=\mu\frac{N\,i_a}{2}\cos(\varphi)\left(\beta_1-\beta_2\cos(2\varphi-2\theta_r)\right) \quad . \tag{1.26}$$

The flux through a winding turn with its magnetic axis at an angle φ from winding a,

$$\begin{aligned}\psi_a&=\int_{\phi-\frac{\pi}{2}}^{\phi+\frac{\pi}{2}} B_r(\xi,\theta_r)rl\,d\xi\\&=r\,l\,\mu N\,i_a\left(\beta_1\cos(\varphi)-\beta_2/2(\cos(\varphi-2\theta_r)-\cos(3\varphi-2\theta_r)/3)\right)\end{aligned} \tag{1.27}$$

To obtain the flux coupling from winding a through winding b, the flux linked from each turn must be summed over the whole winding,

$$\lambda_{ab}=\int N_b(\xi)\Psi_a(\xi,\theta_r)d\xi \quad . \tag{1.28}$$

b's winding distribution is

$$N_b=\frac{N}{2}\cos(\phi-\frac{2\pi}{3}) \tag{1.29}$$

which after some calculation leads to

$$\begin{aligned}\lambda_{ab}&=\int_{\phi_b-\frac{\pi}{2}}^{\phi_b+\frac{\pi}{2}} N_b(\xi)\Psi_a(\xi,\theta_r)d\xi\\&=rl\,\mu\left(\frac{N}{2}\right)^2 i_a\pi\left(-\frac{\beta_1}{2}-\frac{\beta_2}{2}\cos(2\theta_r-\frac{2\pi}{3})\right)\end{aligned} \tag{1.30}$$

The mutual inductance L_{ab} is obtained by dividing by i_a. To express this equation in the same form as the other inductances, compare it with the self inductance for winding a

$$L_{aa}=L_{ls}+rl\,\mu\left(\frac{N}{2}\right)^2\pi\left(\beta_1-\frac{\beta_2}{2}\cos(2\theta_r)\right) \tag{1.31}$$

which gives

$$L_{ab} = -L/2 - L_{\Delta}\cos(2\theta_r - 2\pi/3) \quad . \tag{1.32}$$

The mutual inductances L_{ac} and L_{bc} are calculated in a similar way.

$$L_{ac} = -L/2 - L_{\Delta}\cos(2\theta_r + 2\pi/3) \tag{1.33}$$

$$L_{bc} = -L/2 - L_{\Delta}\cos(2\theta_r) \tag{1.34}$$

The above derivations lead to the following inductance matrix,

$$\boldsymbol{L}_s(\theta_r) = \begin{bmatrix} L_{ls} + L - L_{\Delta}\cos(2\theta_r) & -\frac{L}{2} - L_{\Delta}\cos(2\theta_r - \frac{2\pi}{3}) & -\frac{L}{2} - L_{\Delta}\cos(2\theta_r + \frac{2\pi}{3}) \\ -\frac{L}{2} - L_{\Delta}\cos(2\theta_r - \frac{2\pi}{3}) & L_{ls} + L - L_{\Delta}\cos(2\theta_r + \frac{2\pi}{3}) & -\frac{L}{2} - L_{\Delta}\cos(2\theta_r) \\ -\frac{L}{2} - L_{\Delta}\cos(2\theta_r + \frac{2\pi}{3}) & -\frac{L}{2} - L_{\Delta}\cos(2\theta_r) & L_{ls} + L - L_{\Delta}\cos(2\theta_r - \frac{2\pi}{3}) \end{bmatrix} . \tag{1.35}$$

With this inductance matrix the machine flux originating from the stator currents is, $\boldsymbol{L}_s\boldsymbol{i}_{abc}$.

Permanent Magnet

The flux linkage from the permanent magnet is

$$\boldsymbol{\lambda}_m = \lambda_m \begin{bmatrix} \sin(\theta_r) \\ \sin(\theta_r - \frac{2\pi}{3}) \\ \sin(\theta_r + \frac{2\pi}{3}) \end{bmatrix} \quad . \tag{1.36}$$

Mechanical equation

Both the inductance matrix and the permanent magnet flux linkage depend on rotor position. Therefore, the mechanical equations of the rotor must be included in the motor model to have a complete description of the motor.

Using Newton's law

$$J\frac{d_{\omega m}}{dt} = T_e - T_L \quad , \tag{1.37}$$

where J is the inertia of the rotor plus load, T_e the motor torque, T_L load torque and

$\omega_m = d\theta_m/dt$. Torque is change in energy per change in angle, thus, using the coenergy [8]

$$W_c = \frac{1}{2}\boldsymbol{i}_{abc}^T \boldsymbol{L}_s \boldsymbol{i}_{abc} + \boldsymbol{i}_{abc}^T \boldsymbol{\lambda}_m + W_{pm} \quad , \tag{1.38}$$

the torque produced by the machine is

$$T_e = \frac{dW_c}{d\theta_m} \quad . \tag{1.39}$$

The evaluation will be postponed.

1.2 Transformation to qdØ-frame

Now there is a set of equations which describe the motor. These equations though, depend on rotor position and make the equation system quite involved to solve.
If the variables are transformed into a reference frame rotating with the rotor, inductance will no longer depend on rotor position. This is because in a reference frame attached to the rotor, reluctance which, in the abc-frame, depends on rotor position will be constant. The transformation used is called the *Park Transform*.

Let $\boldsymbol{K}_s$ be the Park transform.

$$\begin{bmatrix} S_q \\ S_d \\ S_\emptyset \end{bmatrix} = \boldsymbol{K}_s \begin{bmatrix} S_a \\ S_b \\ S_c \end{bmatrix} \quad , \tag{1.40}$$

where S represents voltage, current, etc. in the respective domains. q, d and $\emptyset$, stands for quadrature, direct and zero-sequence variables, respectively.

$\boldsymbol{K}_s$ is defined as

$$\boldsymbol{K}_s \equiv \frac{2}{3}\begin{bmatrix} \cos\theta & \cos(\theta - \frac{2\pi}{3}) & \cos(\theta + \frac{2\pi}{3}) \\ \sin\theta & \sin(\theta - \frac{2\pi}{3}) & \sin(\theta + \frac{2\pi}{3}) \\ \frac{1}{2} & \frac{1}{2} & \frac{1}{2} \end{bmatrix} \quad , \tag{1.41}$$

and its inverse as

$$\boldsymbol{K}_s^{-1}=\begin{bmatrix} \cos\theta & \sin\theta & 1 \\ \cos(\theta-\frac{2\pi}{3}) & \sin(\theta-\frac{2\pi}{3}) & 1 \\ \cos(\theta+\frac{2\pi}{3}) & \sin(\theta-\frac{2\pi}{3}) & 1 \end{bmatrix} \quad . \tag{1.42}$$

In $\boldsymbol{K}_s$ there is a factor of 2/3 in front of the matrix. This factor can be understood by the discussion about the mmf-wave. For a balanced set of, say, voltages, the resultant voltage vector has amplitude 3/2 times that of the individual amplitudes. The factor 2/3 makes the amplitude of quantities expressed in the qd-frame correspond to that of each individual phase in the stator abc-frame.
The last row in $\boldsymbol{K}_s$ is the zero sequence. If we consider current and the neutral point of the motor is grounded, then $i_\emptyset$ is the current flowing from neutral to ground. Normally motors are operated with the neutral point floating and so, there is no need to consider the zero sequence.
Another feature that may be noted with the above definition of the Park Transform, it is not power invariant. This is because $\det(\boldsymbol{K}_s) \neq 1$.

Let

$$P_{qd\emptyset}=\langle \boldsymbol{v}_{qd\emptyset}, \boldsymbol{i}_{qd\emptyset} \rangle = w_1 v_q i_q + w_2 v_d i_d + w_3 v_\emptyset i_\emptyset \tag{1.43}$$

The input power in the abc-frame is

$$P_{abc}=\boldsymbol{v}_{abc}\cdot\boldsymbol{i}_{abc}=\boldsymbol{v}_{abc}^T\boldsymbol{i}_{abc} \quad . \tag{1.44}$$

Transform the abc-variables to the qdØ-frame and use the fact that power must be equal in both reference frames,

$$\begin{aligned} P_{abc}&=\boldsymbol{v}_{abc}^T\boldsymbol{i}_{abc}=(\boldsymbol{K}_s^{-1}\boldsymbol{v}_{qd\emptyset})^T\boldsymbol{K}_s^{-1}\boldsymbol{i}_{qd\emptyset}=\boldsymbol{v}_{qd\emptyset}\boldsymbol{K}_s^{-T}\boldsymbol{K}_s^{-1}\boldsymbol{i}_{qd\emptyset} \\ &=\boldsymbol{v}_{qd\emptyset}\begin{bmatrix} \frac{3}{2} & 0 & 0 \\ 0 & \frac{3}{2} & 0 \\ 0 & 0 & 3 \end{bmatrix}\boldsymbol{i}_{qd\emptyset}=\frac{3}{2}\left(v_q i_q + v_d i_d + 2 v_\emptyset i_\emptyset\right)=P_{qd\emptyset} \quad . \end{aligned} \tag{1.45}$$

$\Rightarrow$

$$P_{qd\emptyset}=\langle \boldsymbol{v}_{qd\emptyset}, \boldsymbol{i}_{qd\emptyset} \rangle = \frac{3}{2} v_q i_q + \frac{3}{2} v_d i_d + 3 v_\emptyset i_\emptyset \tag{1.46}$$

We are now going to transform $\boldsymbol{V}_{abc}$, first to an arbitrary qdØ reference frame, and then let this transformation be attached to the rotor.

Express $\boldsymbol{v}_{abc}$ in qdØ-variables,

$$\boldsymbol{v}_{abc} = \boldsymbol{R}_s \boldsymbol{i}_{abc} + \frac{d}{dt}\boldsymbol{\Lambda}_{abc} = \boldsymbol{R}_s \boldsymbol{K}_s^{-1} \boldsymbol{i}_{qd\emptyset} + \frac{d}{dt}(\boldsymbol{K}_s^{-1}\boldsymbol{\Lambda}_{qd\emptyset}) \quad , \tag{1.47}$$

and transform $\boldsymbol{v}_{abc}$ into $\boldsymbol{v}_{qd\emptyset}$,

$$\boldsymbol{v}_{qd\emptyset} = \boldsymbol{K}_s \boldsymbol{R}_s \boldsymbol{K}_s^{-1} \boldsymbol{i}_{qd\emptyset} + \boldsymbol{K}_s \frac{d}{dt}(\boldsymbol{K}_s^{-1}\boldsymbol{\Lambda}_{qd\emptyset}) \quad . \tag{1.48}$$

The resistance does not change when transformed since,

$$\boldsymbol{K}_s \boldsymbol{R}_s \boldsymbol{K}_s^{-1} = \boldsymbol{K}_s r_s \boldsymbol{I}\, \boldsymbol{K}_s^{-1} = r_s \boldsymbol{K}_s \boldsymbol{K}_s^{-1} = \boldsymbol{R}_s \quad . \tag{1.49}$$

The second term

$$\boldsymbol{K}_s \frac{d}{dt}(\boldsymbol{K}_s^{-1}\boldsymbol{\Lambda}_{qd\emptyset}) = \boldsymbol{K}_s \left(\left(\frac{d}{dt}\boldsymbol{K}_s(\theta_T) \right) \boldsymbol{\Lambda}_{qd\emptyset} + \boldsymbol{K}_s^{-1} \frac{d}{dt}\boldsymbol{\Lambda}_{qd\emptyset}(\theta_T, \theta_r) \right) \tag{1.50}$$

$$\boldsymbol{K}_s(\theta_T) \frac{d}{dt}\boldsymbol{K}_s(\theta_T) = \omega_T \begin{bmatrix} 0 & 1 & 0 \\ -1 & 0 & 0 \\ 0 & 0 & 0 \end{bmatrix} \tag{1.51}$$

$$\boldsymbol{K}_s \frac{d}{dt}(\boldsymbol{K}_s^{-1}\boldsymbol{\Lambda}_{qd\emptyset}) = \omega_T \begin{bmatrix} \lambda_d \\ -\lambda_q \\ 0 \end{bmatrix} + \frac{d}{dt}\boldsymbol{\Lambda}_{qd\emptyset} \tag{1.52}$$

Voltage equations in the arbitrary frame

$$\boldsymbol{v}_{qd\emptyset} = \boldsymbol{R}_s \boldsymbol{i}_{qd\emptyset} + \omega_T \begin{bmatrix} \lambda_d \\ -\lambda_q \\ 0 \end{bmatrix} + \frac{d}{dt}\boldsymbol{\Lambda}_{qd\emptyset} \tag{1.53}$$

Now we want to express flux, $\boldsymbol{\Lambda}_{qd\emptyset}$, in component form.
First expand $\boldsymbol{\Lambda}_{abc}$,

$$\boldsymbol{\Lambda}_{abc} = \boldsymbol{L}_s \boldsymbol{i}_{abc} + \boldsymbol{\lambda}_m = \boldsymbol{L}_s \boldsymbol{K}_s^{-1} \boldsymbol{i}_{qd\emptyset} + \boldsymbol{\lambda}_m \tag{1.54}$$

$\Rightarrow$

$$\boldsymbol{\Lambda}_{qd\emptyset} = \boldsymbol{K}_s \boldsymbol{L}_s \boldsymbol{K}_s^{-1} \boldsymbol{i}_{qd\emptyset} + \boldsymbol{K}_s \boldsymbol{\lambda}_m \tag{1.55}$$

$$\boldsymbol{K}_s \boldsymbol{L}_s(\theta_r) \boldsymbol{K}_s^{-1} = \begin{bmatrix} L_{ls} + \frac{3}{2}\left(L - L_\Delta \cos(2\theta_T - 2\theta_r)\right) & -\frac{3}{2} L_\Delta \sin(2\theta_T - 2\theta_r) & 0 \\ -\frac{3}{2} L_\Delta \sin(2\theta_T - 2\theta_r) & L_{ls} + \frac{3}{2}\left(L + L_\Delta \cos(2\theta_T - 2\theta_r)\right) & 0 \\ 0 & 0 & L_{ls} \end{bmatrix} \tag{1.56}$$

$$\boldsymbol{K}_s(\theta_T) \boldsymbol{\lambda}_m(\theta_r) = \lambda_m \begin{bmatrix} -\sin(\theta_T - \theta_r) \\ \cos(\theta_T - \theta_r) \\ 0 \end{bmatrix} \tag{1.57}$$

For a single phase machine

$$L_{mq} = L - L_\Delta \quad \text{and} \quad L_{md} = L + L_\Delta \quad .$$

For a three phase machine the space mmf wave has amplitude 3/2 times that of each individual phase which gives,

$$L_{mq} = \frac{3}{2}(L - L_\Delta) \quad \text{and} \quad L_{md} = \frac{3}{2}(L + L_\Delta) \tag{1.58}$$

$\Rightarrow$

$$L = \frac{1}{3}(L_{md} + L_{mq}) \quad \text{and} \quad L_\Delta = \frac{1}{3}(L_{md} - L_{mq}) \quad . \tag{1.59}$$

Flux linkage in qdØ coordinates may therefore be expressed as

$$\boldsymbol{\Lambda}_{qd\emptyset} = \begin{bmatrix} \frac{L_d + L_q}{2} - \frac{L_d - L_q}{2}\cos(2\theta_T - 2\theta_r) & -\frac{L_d - L_q}{2}\sin(2\theta_T - 2\theta_r) & 0 \\ -\frac{L_d - L_q}{2}\sin(2\theta_T - 2\theta_r) & \frac{L_d + L_q}{2} + \frac{L_d - L_q}{2}\cos(2\theta_T - 2\theta_r) & 0 \\ 0 & 0 & L_{ls} \end{bmatrix} \begin{bmatrix} i_q \\ i_d \\ i_\emptyset \end{bmatrix} + \lambda_m \begin{bmatrix} -\sin(\theta_T - \theta_r) \\ \cos(\theta_T - \theta_r) \\ 0 \end{bmatrix} \quad , \tag{1.60}$$

where $L_q = L_{ls} + L_{mq}$ and $L_d = L_{ls} + L_{md}$. θ_T is the angle which rotates the transformed reference frame and θ_r the rotor position in electrical radians. This is the flux expressed in the arbitrary reference frame.

If the reference frame rotates in synchronism with the rotor and both angles have the same initial conditions then $\theta_T = \theta_r$, and total flux in the rotor reference frame becomes,

$$\boldsymbol{\Lambda}^r_{qd\emptyset} = \begin{bmatrix} L_q & 0 & 0 \\ 0 & L_d & 0 \\ 0 & 0 & L_{ls} \end{bmatrix} \begin{bmatrix} i^r_q \\ i^r_d \\ i^r_\emptyset \end{bmatrix} + \begin{bmatrix} 0 \\ \lambda_m \\ 0 \end{bmatrix} \quad . \tag{1.61}$$

Stator voltage expressed in the rotor qdØ-frame then is,

$$\boldsymbol{v}^r_{qd\emptyset} = \boldsymbol{R}_s \boldsymbol{i}^r_{qd\emptyset} + \omega_r \begin{bmatrix} \lambda_d \\ -\lambda_q \\ 0 \end{bmatrix} + \frac{d}{dt} \boldsymbol{\Lambda}^r_{qd\emptyset} \quad , \tag{1.62}$$

and in expanded form

$$\begin{aligned} v^r_q &= (r_s + pL_q) i^r_q + \omega_r L_d i^r_d + \omega_r \lambda_m \\ v^r_d &= (r_s + pL_d) i^r_d - \omega_r L_q i^r_q \\ v^r_\emptyset &= (r_s + pL_{ls}) i^r_\emptyset \end{aligned} \tag{1.63}$$

where $p = d/dt$.

Now let's return to the torque equation.

$$W_c = \frac{1}{2} \boldsymbol{i}^T_{abc} \boldsymbol{L}_s \boldsymbol{i}_{abc} + \boldsymbol{i}^T_{abc} \boldsymbol{\lambda}_m + W_{pm} \quad . \tag{1.64}$$

$$T_e = \frac{dW_c}{d\theta_m} = \frac{P}{2} \frac{dWc}{d\theta_r} = \frac{P}{2} \left(\frac{1}{2} \boldsymbol{i}^T_{abc} \frac{d}{d\theta_r} \boldsymbol{L}_s \boldsymbol{i}_{abc} + \boldsymbol{i}^T_{abc} \frac{d}{d\theta_r} \boldsymbol{\lambda}_m \right) \tag{1.65}$$

making a change of variables, $\boldsymbol{i}_{abc} = \boldsymbol{K}^{-1}{}_s \, \boldsymbol{i}_{qd\emptyset}$,

$$\begin{aligned} T_e &= \frac{P}{2} \left(\frac{1}{2} (K^{-1}_s \boldsymbol{i}_{qd\emptyset})^T \frac{d}{d\theta_r} \boldsymbol{L}_s \boldsymbol{K}^{-1}_s \boldsymbol{i}_{qd\emptyset} + (\boldsymbol{K}^{-1}_s \boldsymbol{i}_{qd\emptyset})^T \frac{d}{d\theta_r} \boldsymbol{\lambda}_m \right) \\ &= \frac{P}{2} \left(\frac{1}{2} \boldsymbol{i}^T_{qd\emptyset} \boldsymbol{K}^{-T}_s \frac{d}{d\theta_r} \boldsymbol{L}_s \boldsymbol{K}^{-1}_s \boldsymbol{i}_{qd\emptyset} + \boldsymbol{i}^T_{qd\emptyset} \boldsymbol{K}^{-T}_s \frac{d}{d\theta_r} \boldsymbol{\lambda}_m \right) \end{aligned} \tag{1.66}$$

$$\boldsymbol{K}^{-T}_s(\theta_T) \frac{d}{d\theta_r} \boldsymbol{L}_s(\theta_r) \boldsymbol{K}^{-1}_s(\theta_T) = \frac{9}{2} \begin{bmatrix} -\sin(2\theta_T - 2\theta_r) & \cos(2\theta_T - 2\theta_r) & 0 \\ \cos(2\theta_T - 2\theta_r) & \sin(2\theta_T - 2\theta_r) & 0 \\ 0 & 0 & 0 \end{bmatrix} \tag{1.67}$$

$$\boldsymbol{K}^{-T}_s(\theta_T) \frac{d}{dr} \boldsymbol{\lambda}_m(\theta_r) = \frac{3}{2} \lambda_m \begin{bmatrix} \cos(\theta_T - \theta_r) \\ \sin(\theta_T - \theta_r) \\ 0 \end{bmatrix} \tag{1.68}$$

$\Rightarrow$

$$T_e = \frac{P}{2}\left(\frac{9}{4} L_\Delta \boldsymbol{i}_{qd\emptyset}^T \begin{bmatrix} -\sin(2\theta_T - 2\theta_r) & \cos(2\theta_T - 2\theta_r) & 0 \\ \cos(2\theta_T - 2\theta_r) & \sin(2\theta_T - 2\theta_r) & 0 \\ 0 & 0 & 0 \end{bmatrix} \boldsymbol{i}_{qd\emptyset} + \frac{3}{2} \lambda_m \boldsymbol{i}_{qd\emptyset}^T \begin{bmatrix} \cos(\theta_T - \theta_r) \\ \sin(\theta_T - \theta_r) \\ 0 \end{bmatrix} \right) \tag{1.69}$$

If this result is compared with eq. (1.60) one obtain the following torque equation

$$T_e = \frac{3P}{4}\left(\lambda_d i_q - \lambda_q i_d \right) \quad . \tag{1.70}$$

The above equation is true for all reference frames expressed in qdØ coordinates. If instead we use the rotor frame and substitute λ_d and λ_q from eq. (1.61), then

$$T_e = \frac{3P}{4}\left((L_d - L_q) i_q^r i_d^r + \lambda_m i_q^r \right) \quad . \tag{1.71}$$

The first term is due to reluctance variations and disappears in a salient free machine. The second term is due to the permanent magnet flux.

These equations describe the electromechanical behavior of the machine in the qdØ domain. The set of equations given in rotor reference are repeated below:

$$v_q^r = (r_s + pL_q) i_q^r + \omega_r L_d i_d^r + \omega_r \lambda_m \tag{1.72}$$

$$v_d^r = (r_s + pL_d) i_d^r - \omega_r L_q i_q^r \tag{1.73}$$

$$v_\emptyset^r = (r_s + pL_{ls}) i_\emptyset^r \tag{1.74}$$

$$T_e = \frac{3P}{4}\left((L_q - L_d) i_q^r i_d^r + \lambda_m i_q^r \right) \tag{1.75}$$

$$J \frac{d\omega_r}{dt} = \frac{P}{2}\left(T_e - T_L \right) \tag{1.76}$$

Summary

In this chapter the motor model was derived. The last set of equations expressed in the rotor reference frame is used to model the motor in simulations. The inductance matrix, $\boldsymbol{L}_s$, which describe the self and mutual flux coupling of the stator windings, depends on rotor position. Therefore the motor equations were transformed to a new coordinate system in which the inductance matrix becomes constant when the coordinate system rotates in synchronism with the rotor. The motor model expressed in this new coordinate system called the *qdØ-frame* is more manageable than when expressed in the natural motor variables. However, the resulting differential equations are still highly nonlinear and require a computer to solve for the transient behavior.

Chapter 2 Some common control schemes for PM motors

In this chapter a short summary of some common control techniques used for PM motor control are presented [22]. PMSM control techniques can be divided into scalar and vector control. Scalar control is based on relationships valid in steady-state. Amplitude and frequency of the controlled variables are considered. In vector control amplitude and position of a controlled space vector is considered. These relationships are valid even during transients which is essential for precise torque and speed control.

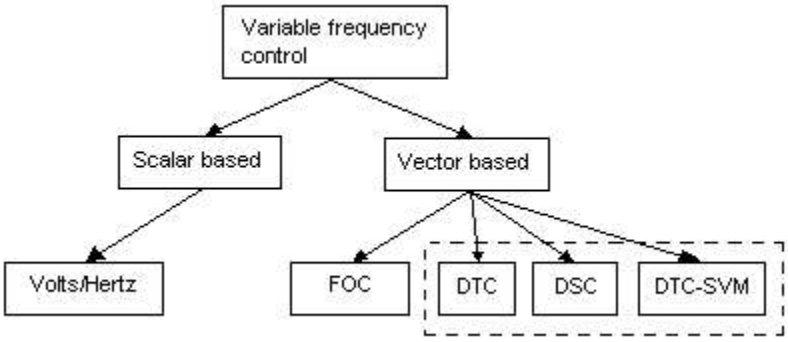

Figure 2.1, Some common control techniques used for PMSM.
Control methods in the dashed box belong to the DTC family.

2.1 Scalar control

Scalar control is based on relationships valid in steady state. Only magnitude and frequency of voltage, current, etc. are controlled. Scalar control is used e.g. where several motors are driven in parallel by the same inverter.

2.1.1 Volts/Hertz control

Volts/Hertz control is among the simplest control schemes for motor control. The control is an open-loop scheme and does not use any feedback loops.
The idea is to keep stator flux constant at rated value so that the motor develops rated torque/ampere ratio over its entire speed range.

The voltage equations for a permanent magnet motor were derived in chapter 1. In qd-coordinates these equations are

$$v_q = r_s i_q + \omega \lambda_d + \frac{d}{dt}\lambda_q \qquad (2.1)$$

$$v_d = r_s i_d - \omega\lambda_q + \frac{d}{dt}\lambda_d \quad (2.2)$$

where v_q and v_d are stator voltage, r_s stator resistance, i stator current, ω angular velocity and λ is the flux linkage.
In stationarity the derivative terms disappears, furthermore, if speed is high the emf voltage, $\omega\lambda$, is relatively high and the resistive voltage drop may be ignored.
In this case, if stator flux is to be kept constant, the voltage applied should be directly proportional to the rotor angular frequency.
At lower speeds an extra boost voltage is applied to compensate for the resistive drop. The principle is valid only for stationarity when the derivative terms vanish.

2.2 Vector control

The problem with scalar control is that motor flux and torque in general are coupled. This inherent coupling affects the response and makes the system prone to instability if it is not considered. In vector control, not only the magnitude of the stator and rotor flux is considered but also their mutual angle.

2.2.1 Field Oriented Control

The vector control of currents and voltages results in control of the spatial orientation of the electromagnetic fields in the machine and has led to the name *field orientation*.
Field Oriented Control usually refers to controllers which maintain a 90º electrical angle between rotor and stator field components. Systems which depart from the 90º orientation are referred to as *field angle control* or *angle control* [3].

In a DC motor the field flux, which in this case is the stator flux, and the armature flux (rotor) are held orthogonal mechanically by the commutator. When the fields are orthogonal, armature flux does not affect the field flux and the motor torque responds immediately to a change in armature flux or equivalently, armature current. In an AC motor the field flux (which now is in the rotor) rotates, but in a FOC the controller rotates the armature (stator) flux so that armature and field flux are kept orthogonal, and hence, the AC motor behaves as a DC motor. The requirements are,

1. Independently controlled armature current to overcome the effects of winding resistance, leakage inductance and induced voltage.
2. Independently controlled or constant field flux.
3. Independently controlled orthogonal spatial angle (electrical) between stator and rotor flux.

A vector controlled PM motor is also known as a *brushless DC-machine*.

To see how the principle works, observe that the currents in the qd rotor reference frame may be written as

$$i_q^r = i_s \cos(\varphi),\ i_d^r = i_s \sin(-\varphi) = -i_s \sin(\varphi),$$

where i_s is the absolute value of the current vector $\boldsymbol{i}_{qd}$.

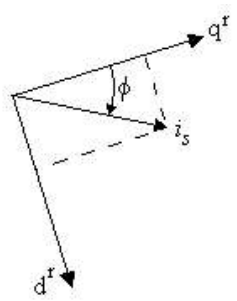

Figure 2.2

The current and torque equations in the rotor reference frame are,

$$-L_q \frac{d}{dt} i_q^r = r_s i_q^r + \omega_r L_d i_d^r + \omega_r \lambda_m - v_q^r \tag{2.3}$$

$$-L_d \frac{d}{dt} i_d^r = r_s i_d^r - \omega_r L_q i_q^r - v_d^r \tag{2.4}$$

$$T_e = \frac{3P}{4}\left((L_d - L_q) i_q^r i_d^r + \lambda_m i_q^r\right) \tag{2.5}$$

where v^r_q and v^r_d are considered inputs.
According to requirement 3, the angle between stator and rotor field flux should be kept at 90º, i.e. φ = 0, which leads to

$$i_q^r = i_s,\ i_d^r = 0$$

and

$$-L_q \frac{d}{dt} i_q^r = r_s i_q^r + \omega_r \lambda_m - v_q^r \tag{2.6}$$

$$i_d^r = 0 | v_d^r = -\omega_r L_q i_q^r \tag{2.7}$$

$$T_e = \frac{3P}{4} \lambda_m i_q^r \tag{2.8}$$

Hence the torque is directly proportional to $i^r_q = i_s$, which in turn is controlled as fast as equation (2.6) allows.

2.2.2 Direct Torque Control

The principle of Direct Torque Control (DTC) is to directly select voltage vectors according to the difference between reference and actual value of torque and flux linkage. Torque and flux errors are compared in hysteresis comparators. Depending on the comparators a voltage vector is selected from a table.
Advantages of the DTC are low complexity and that it only need to use of one motor parameter, the stator resistance. No pulse width modulation is needed; instead one of the six VSI voltage vectors is applied during the whole sample period. All calculations are done in a stationary reference frame which does not involve the explicit knowledge of rotor position. Still, for a synchronous motor, rotor position must be known at start-up. The DTC hence require low computational power when implemented digitally.
The system possess good dynamic performance but shows quite poor performance in steady-state since the crude voltage selection criteria give rise to high ripple levels in stator current, flux linkage and torque.
Its simplicity makes it possible to execute every computational cycle in a short time period and use a high sample frequency. For every doubling in sample frequency, the ripple will approximately halve. The problem is that the power switches used in the inverter impose a limit for the maximum sample frequency.

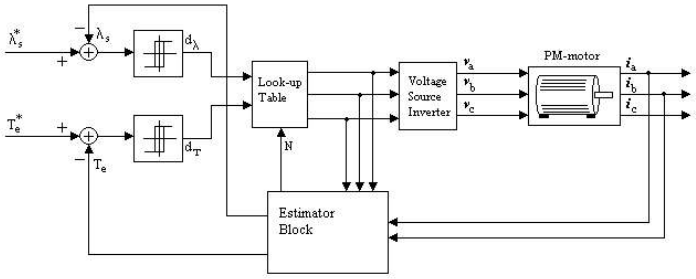

Figure 2.3, DTC block diagram

In the next chapter a more detailed description the DTC is presented and some problems are illuminated, some of which are treated further in chapter 4 where an improved variant of the DTC scheme is presented.

2.2.3 Direct Self Control

Direct Self Control (DSC) is very similar to the DTC scheme presented above. It can be shown that the DSC can be considered a special case of the DTC [13,22].

Some of the characteristics of DSC are:
1. Inverter switching frequency is lower than in the DTC scheme.
2. Excellent torque dynamics both in constant flux and in field weakening regions.

Low switching frequency and fast torque control over the whole operating range makes DSC preferable over DTC in high power traction systems.

2.2.4 DTC – Space Vector Modulation

In the DTC system the same active voltage vector is applied during the whole sample period, and possibly several consecutive sample intervals which give rise to relatively high ripple levels in stator current, flux linkage and torque.
One of the proposals to minimize these problems is to introduce Space Vector Modulation. SVM is a pulse width modulation technique able to synthesize any voltage vector lying inside the sextant spanned by the six VSI voltage vectors.

In the DTC – SVM scheme the hysteresis comparators are replaced by an estimator which calculates an appropriate voltage vector to compensate for torque and flux errors. This method has proved to generate very low torque and flux ripple while showing almost as good dynamic performance as the DTC system. The DTC-SVM system, though being a good performer, introduces more complexity and lose an essential feature of the DTC, its simplicity.

Summary

This chapter presents some of the control techniques used for PM motor control. A scalar control technique called Volts/Hertz control being among the simplest control methods. It is used where exact torque and flux control is not essential but where speed control is desirable, like when several motors are driven in parallel by a single inverter.
Vector control is used where high performance torque and flux control is needed. There are different ways to implement vector control. FOC, DTC, DSC and DTC with space vector modulation are some of the techniques. DTC and DSC are simple, robust and offer good dynamic performance. FOC and DTC-SVM gives the best performance in terms of ripple levels but requires more processor power and are more complicated to implement.

Chapter 3 Direct Torque Control

In most control systems as in Field Oriented Control, the control algorithm calculates a control signal whose amplitude depends on the difference between desired and actual value. This control signal can assume any value in a given interval.
In Direct Torque Control the control algorithm chose a control signal that increases the quantity in question if actual value is lower than desired and vice versa. Whether the difference is big or small the same control signal is chosen.

There are three signals which affect the control action in a DTC system; torque, flux linkage and the angle of the resultant flux linkage vector.
One revolution is divided into six sectors. In each sector the DTC chose between 4 voltage vectors. Both flux and torque errors are compared in 2-level hysteresis comparators.
Two of the vectors increase and the other two decrease torque. Another pair of vectors increase and decrease flux. For each combination of the torque and flux hysteresis comparator states there is only one of the four voltage vectors which at the same time compensate torque and flux as desired.

The chapter first presents the different blocks in a DTC system. In section 3.2 and 3.3 the effects of a voltage vector on torque and flux is analyzed based on [11,12,13]. In section 3.4 some of the problems encountered in a DTC system are mentioned [23].

3.1 The Direct Torque Control system

The DTC system was first mentioned in chapter 2 in connection with some other control strategies. In this section the DTC control system is presented in detail and the functions of all system blocks are explained.

Figure 3.1 show the block diagram of the DTC. Each block is described in detail below.

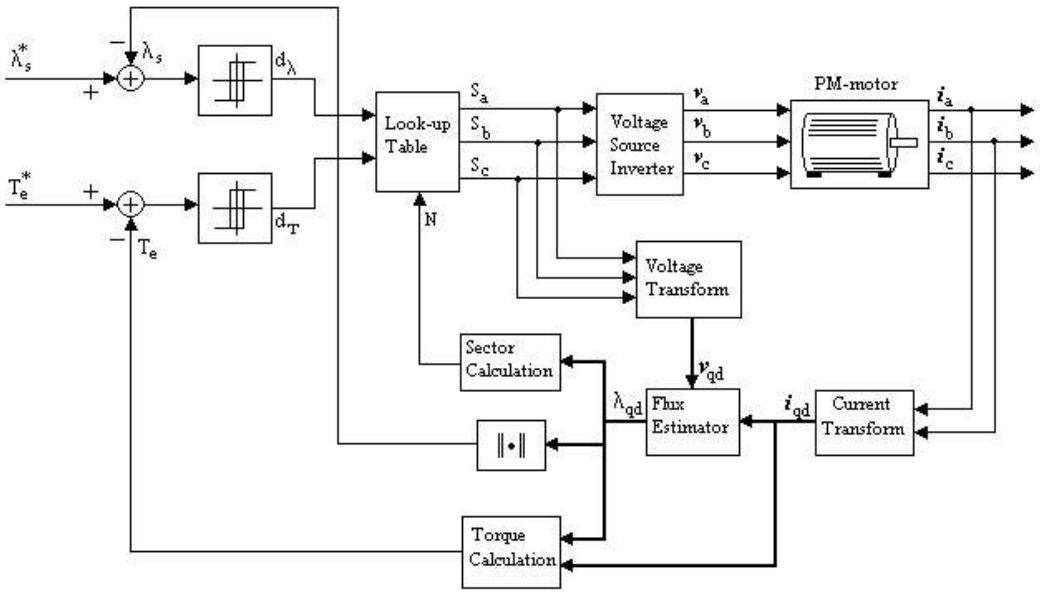

Figure 3.1, The different blocks in a DTC system

Let's start with the motor currents and follow the signals around the system to the Voltage Source Inverters output.

Current Transform

As seen in the figure only two of the input currents are sensed. The motor in a drive system is normally operated with its neutral point floating, in this case $i_a + i_b + i_c = 0$ so the current not sensed is given of them other two. The $\boldsymbol{i}_{abc}$ current is then transformed to its quadrature and direct axes components according to the Park Transformation presented in chapter one.
In chapter one the qd-components were transformed into the rotor reference frame and absolute rotor position was supposed to be known. In reality there is a desire of not using rotor position explicitly because this implies the use of angular encoders. In the DTC system, variables are transformed into the qd stator reference frame, which does not make use of any angular information.

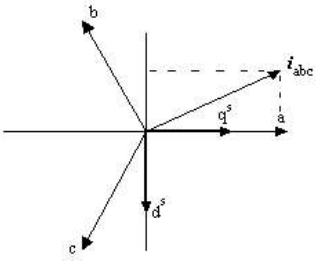

Figure 3.2

This transformation becomes a simple mapping,

$$\begin{bmatrix} i_q^s \\ i_d^s \end{bmatrix} = \begin{bmatrix} \frac{2}{3} & -\frac{1}{3} & -\frac{1}{3} \\ 0 & -\frac{1}{\sqrt{3}} & \frac{1}{\sqrt{3}} \end{bmatrix} \begin{bmatrix} i_a \\ i_b \\ i_c \end{bmatrix} \tag{3.1}$$

The zero component is left out since, when the neutral floats there is no need to consider it.

Flux Estimator

Now that the current, $\boldsymbol{i}_{qd}$, is known, the signal continues into the flux estimator. Into this block also enters the VSI voltage vector transformed, as the current, to the qd-stationary reference frame. The voltage, $\boldsymbol{v}_{qd}$, is calculated as in eq. (3.1), so no further explanation is needed.
From eq. (1.53) with the zero component left out,

$$\boldsymbol{v}_{qd} = \boldsymbol{R}_s \boldsymbol{i}_{qd} + \omega_T \begin{bmatrix} \lambda_d \\ -\lambda_q \end{bmatrix} + \frac{d}{dt} \boldsymbol{\Lambda}_{qd} \tag{3.2}$$

one directly obtain a means for stator flux estimation by noting that $\omega_T = 0$ and rearranging,

$$\boldsymbol{\Lambda}_{qd}^s = \int (\boldsymbol{v}_{qd}^s - \boldsymbol{R}_s \boldsymbol{i}_{qd}^s)\, dt \tag{3.3}$$

This formula is the foundation for implementing the flux estimator. It may be implemented directly, or approximated by various methods to avoid integrator drift [23].

Sector Calculation

The control action taken by the DTC control is based on the states of the flux and torque hysteresis comparators. Flux is increased by applying a vector pointing in the flux Λ^s_{qd}-direction and torque is increased by applying a vector pointing in the rotational direction. In order to do this, the angular position of the stator flux vector must be known so that the DTC can chose between an appropriate set of vectors depending on the flux position.

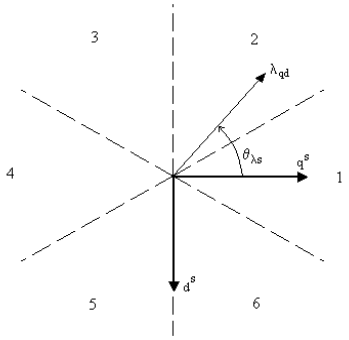

Figure 3.3, DTC sectors and reference axes

Each sector spans 60º degrees; the sectors are numbered as in fig. 3.3.
As seen from the picture the angle $\theta_{\lambda s}$ can be found from

$$\tan(\theta_{\lambda s}) = \frac{-\lambda_d^s}{\lambda_q^s} \tag{3.4}$$

If λ_{qd} belongs to sector 1, switch vectors, u_2, u_3, u_5 and u_6 are used.

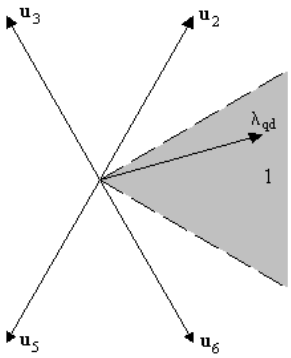

Figure 3.4, VSI vectors used when λ_{qd} is in sector 1

The block under Sector Calculation computes the vector norm before estimated flux, λ_s, is passed on and compared with the command value, λ^*_s.

Torque Calculation

From eq. (1.70),

$$T_e = \frac{3P}{4}\left(\lambda_d i_q - \lambda_q i_d\right) \tag{3.5}$$

which is true for all qd-reference frames. To calculate torque one only has to substitute the corresponding, already, calculated fluxes and currents. Torque calculation is thus a simple operation.

Torque and flux hysteresis comparators

Now we know in which sector is the flux and its norm, and we also know how much torque the motor develops.
Estimated torque and flux are compared to their command values. The difference between command and estimated value is compared in the hysteresis comparators.

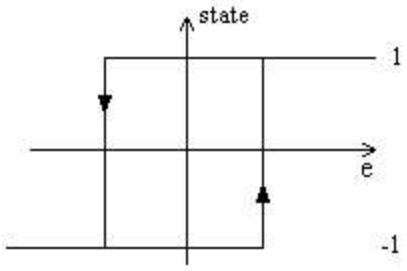

Figure 3.5, 2-level hysteresis comparator

Look-up Table

The hysteresis comparator states, d_T and d_λ, together with the sector number, N, are now used by the Look-up Table block to chose an appropriate voltage vector.
A table frequently used in DTC when controlling a Permanent Magnet motor is shown in table 3.1,

		N					
d_λ	d_T	1	2	3	4	5	6
-1	-1	u_5	u_6	u_1	u_2	u_3	u_4
	1	u_3	u_4	u_5	u_6	u_1	u_2
1	-1	u_6	u_1	u_2	u_3	u_4	u_5
	1	u_2	u_3	u_4	u_5	u_6	u_1

Table 3.1, DTC switch table

A high hysteresis state increases the corresponding quantity, and vice versa. The selected voltage vector is sent to the Voltage Source Inverter in, for the VSI, a suitable format and then synthesized.

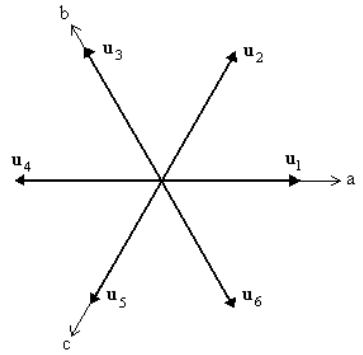

Figure 3.6, VSI voltage vectors and the motor's magnetic axes

Voltage Source Inverter

The VSI synthesizes the voltage vectors commanded by the Look-up Table block. In the case of DTC this task is quite simple since no pulse width modulation is used; the output devices stay in the same state during the entire sample period.

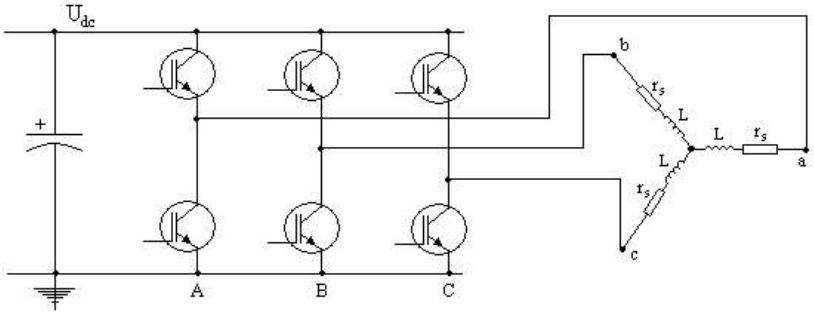

Figure 3.7, VSI and how the motor windings are connected

Figure 3.7 shows a simplified sketch of the VSI output stage, and how the motor windings are connected.
The output-signals from the Look-up Table block in Fig. 3.1 are named S_a, S_b and S_c. These are boolean variables indicating the switch state in the inverter output-branches.

Let $S_i = 1$ when the high or upper switch is on and the lower is off, and $S_i = 0$ when the lower is on and the upper off. The inverter states, (S_a S_b S_c), generating each voltage vector, then, are

$$u_1 = (1\ 0\ 0),\ u_2 = (1\ 1\ 0),\ u_3 = (0\ 1\ 0),\ u_4 = (0\ 1\ 1),\ u_5 = (0\ 0\ 1),\ u_6 = (1\ 0\ 1)$$

3.2. Torque and Flux equations

This chapter is intended to show how applied voltage vectors affect flux and torque. The results will lead to a better understanding of how the switch table is constructed. Also some problems encountered with the DTC control are illuminated. First some additional results to chapter 1 are presented.

In chapter 1 electromagnetic torque was given as

$$T_e = \frac{3P}{4}\left(\lambda_d i_q - \lambda_q i_d\right) \tag{3.6}$$

Let torque be a vector defined by the cross-product between two vectors and following a left/right-hand rule depending on the coordinate system.
As the motors neutral point is floating one does not need to care about the zero-component, hence the motor is modeled in two dimensions, *q* and *d*.
Let's consider the qd coordinate system lying in the abc-plane. This plane is a cross section of the motor.
We now introduce a new coordinate, *z*, pointing as figure 3.8 along the rotor axis.
This new coordinate system, (*q,d,z*), is a left hand system.

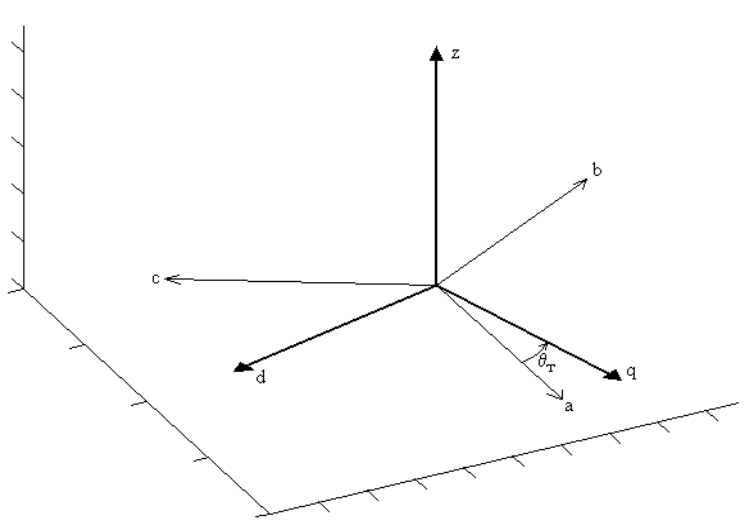

Figure 3.8, Coordinate system

Define the cross-product between two vectors, $\boldsymbol{v}_a = v_{a1}\boldsymbol{e}_q + v_{a2}\boldsymbol{e}_d$ and $\boldsymbol{v}_b = v_{b1}\boldsymbol{e}_q + v_{b2}\boldsymbol{e}_d$, as

$$\boldsymbol{v}_a \times \boldsymbol{v}_b \equiv \begin{vmatrix} \boldsymbol{e}_q & \boldsymbol{e}_d & \boldsymbol{e}_z \\ v_{a1} & v_{a2} & 0 \\ v_{b1} & v_{b2} & 0 \end{vmatrix} = \boldsymbol{e}_z \left(v_{a1} v_{b2} - v_{a2} v_{b1} \right) \tag{3.7}$$

With this definition the torque can be expressed as

$$\boldsymbol{T}_e = \frac{3P}{4} \boldsymbol{i}_{qd} \times \boldsymbol{\lambda}_{qd} \tag{3.8}$$

When analyzing the system different reference frames are convenient. The voltage vectors expressed in the arbitrary reference are,

$$v_q = \frac{2}{3} U_{dc} \cos(\theta_T - \theta_i) \tag{3.9}$$

$$v_d = \frac{2}{3} U_{dc} \sin(\theta_T - \theta_i) \tag{3.10}$$

where θ_i is the angle of the applied voltage vector measured from a's magnetic axis.

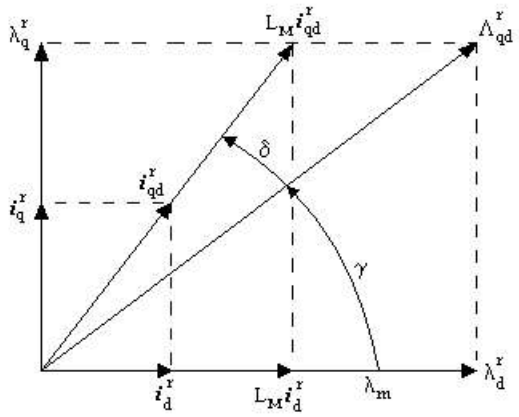

Figure 3.9

γ is the angle between the rotor d-axis and λ_s. From the figure one can see that

$$i_q^r = \lambda_s \sin(\gamma) / L_M \quad . \tag{3.11}$$

Now T_e = 3P/4 $i^r_q \lambda_m$, which gives

$$\sin(\gamma) = \frac{4 T_e L_M}{3 P \lambda_s \lambda_m} \quad . \tag{3.12}$$

δ is the load angle which appear in the torque equation, since

$$\boldsymbol{i}_{qd} \times \boldsymbol{\lambda}_{qd} = i_s \lambda_s \sin(\delta) \quad ,$$

where i_s = abs($\boldsymbol{i}_{qd}$), λ_s = abs($\boldsymbol{\lambda}_{qd}$).

Stator flux equations

Stator flux in the arbitrary qd frame from eq.(1.53) and rearranged, becomes

$$\frac{d}{dt} \boldsymbol{\Lambda}_{qd} = \boldsymbol{v}_{qd} - \boldsymbol{R}_s \boldsymbol{i}_{qd} - \omega_T \begin{bmatrix} \lambda_d \\ -\lambda_q \end{bmatrix} \tag{3.13}$$

For short sample periods

$$\frac{d}{dt} \boldsymbol{\Lambda}_{qd} \approx \frac{\Lambda_{qd}[k+1] - \Lambda_{qd}[k]}{T_s} \tag{3.14}$$

Eq. (3.13) may then be written

$$\lambda_q[\mathrm{k}+1]=T_s\left(v_q[\mathrm{k}]-r_s i_q[\mathrm{k}]-\omega_T \lambda_d[\mathrm{k}]\right)+\lambda_q[\mathrm{k}] \tag{3.15}$$

$$\lambda_d[\mathrm{k}+1]=T_s\left(v_d[\mathrm{k}]-r_s i_d[\mathrm{k}]+\omega_T \lambda_q[\mathrm{k}]\right)+\lambda_d[\mathrm{k}] \tag{3.16}$$

or alternatively eq. (3.13) is rewritten,

$$\lambda_q(t)=\int (v_q-r_s i_q-\omega_T \lambda_d)\,dt \tag{3.17}$$

$$\lambda_d(t)=\int (v_d-r_{sid}+\omega_T \lambda_q)\,dt \tag{3.18}$$

During a sufficiently short time interval, all variables on the right hand side may be approximated constant. Thus,

$$\Delta\lambda_q[\mathrm{k}]=T_s\left(v_q[\mathrm{k}]-r_s i_q[\mathrm{k}]-\omega_T \lambda_d[\mathrm{k}]\right) \tag{3.19}$$

$$\Delta\lambda_d[\mathrm{k}]=T_s\left(v_d[\mathrm{k}]-r_s i_d[\mathrm{k}]+\omega_T \lambda_q[\mathrm{k}]\right) \tag{3.20}$$

Rotor reference

In the rotor reference the equations that describe how flux changes during the next sample period becomes

$$\Delta\lambda_q^r[\mathrm{k}]=T_s\left(v_q^r[\mathrm{k}]-r_s i_q^r[\mathrm{k}]-\omega_r \lambda_d^r[\mathrm{k}]\right) \tag{3.21}$$

$$\Delta\lambda_d^r[\mathrm{k}]=T_s\left(v_d^r[\mathrm{k}]-r_s i_d^r[\mathrm{k}]+\omega_r \lambda_q^r[\mathrm{k}]\right) \tag{3.22}$$

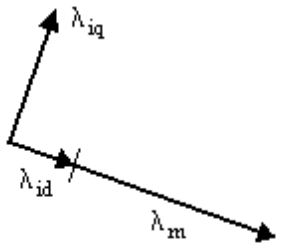

Figure 3.10, Rotor reference flux

Here an interesting property can be seen.
If torque requirement is high i^r_q must be high since this is the variable causing torque in a salient free motor (see eq. 1.71), hence λ^r_q is high. This in turn induces a high positive voltage in the d^r-direction (along the permanent magnet). This voltage increase i^r_d and

hence λ^r_d. A high λ^r_d counteract v^r_q and, when velocity and/or flux are sufficiently high, makes the resultant voltage in the q^r-direction negative which lower λ^r_q or equivalently i^r_q which produced torque.
This short discussion shows that a motor has to be demagnetized when speed is high, in order to work properly. That is, i^r_d must be negative so as to counteract the permanent magnet flux. This operational mode is often referred to as the *flux weakening region.*

λ_s - reference

Assume the qd coordinates rotate in synchronism with the stator flux, and the d-axis is aligned with the flux vector. Then,

$$\Delta \lambda_q^{\lambda_s}[\mathrm{k}] = T_s\left(v_q^{\lambda_s}[\mathrm{k}] - r_s i_q^{\lambda_s}[\mathrm{k}] - \omega_r \lambda_s[\mathrm{k}]\right) \tag{3.23}$$

$$\Delta \lambda_d^{\lambda_s}[\mathrm{k}] = T_s\left(v_d^{\lambda_s}[\mathrm{k}] - r_s i_d^{\lambda_s}[\mathrm{k}]\right) \tag{3.24}$$

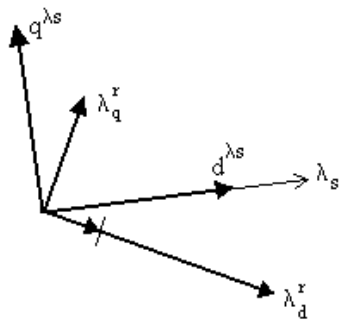

Figure 3.11, λ_s - reference

Stator reference

In the stationary reference frame eq. (3.13) becomes

$$\frac{d}{dt}\boldsymbol{\Lambda}^s_{qd} = \boldsymbol{v}^s_{qd} - \boldsymbol{R}_s \boldsymbol{i}^s_{qd} \tag{3.25}$$

$\Leftrightarrow$

$$\boldsymbol{\Lambda}^s_{qd} = \int (\boldsymbol{v}^s_{qd} - \boldsymbol{R}_s \boldsymbol{i}^s_{qd})\, dt \tag{3.26}$$

The change in flux during one switching period is obtained if the integral is evaluated from t: $t \rightarrow t + T_s$.
Observe that applied voltage is constant during the switching period $\Rightarrow$

$$\Delta \boldsymbol{\Lambda}^s_{qd} = T_s \boldsymbol{v}^s_{qd} - \int \boldsymbol{R}_s \boldsymbol{i}^s_{qd}\, dt \tag{3.27}$$

If the current variation is small between two consecutive samples and furthermore if $r_s i_{qd}$ is small compared to v_{qd}, which is normally the case, then

$$\Delta \boldsymbol{\Lambda}^s_{qd} = T_s \boldsymbol{v}^s_{qd} - T_s \boldsymbol{R}_s \boldsymbol{i}^s_{qd} \tag{3.28}$$

When the resistive voltage drop is low, the last term can be left out. In this case the change in stator flux is directly proportional to amplitude and direction of the applied voltage vector.

$$\Delta \boldsymbol{\Lambda}^s_{qd} = T_s \boldsymbol{v}^s_{qd} \tag{3.29}$$

Here another feature of the PM motor may be noted.
Since the permanent magnet always produce a flux linkage through the stator windings, flux moves even if a zero voltage vector is applied whenever the rotor evolves [16,17]. This is contrary to an induction motor where stator flux is kept almost fixed in amplitude and space when a zero voltage vector is applied.
For very short time periods, though, the permanent magnet is almost fixed in space.

Torque equations

From eq. (3.8) torque can be expressed as

$$T_e = \frac{3P}{4} \boldsymbol{i}_{qd} \times \boldsymbol{\lambda}_{qd} \quad . \tag{3.30}$$

Differentiate eq. (3.30),

$$\frac{d}{dt} T_e = \frac{3P}{4} \left(\frac{d}{dt} \boldsymbol{i}_{qd} \times \boldsymbol{\lambda}_{qd} + \boldsymbol{i}_{qd} \times \frac{d}{dt} \boldsymbol{\lambda}_{qd} \right) \tag{3.31}$$

From eqs. (1.61) and (1.62) for a non-salient motor

$$\frac{d}{dt} \boldsymbol{i}^r_{qd} = \frac{1}{L_M} \left(\boldsymbol{v}^r_{qd} - \boldsymbol{R}_s \boldsymbol{i}^r_{qd} - \omega_r \begin{bmatrix} \lambda^r_d \\ -\lambda^r_q \end{bmatrix} \right) \tag{3.32}$$

If we now substitute eqs. (3.13) and (3.32) into eq.(3.31) and making use of the cross-product and torque equation (3.30), one obtains

$$\frac{d}{dt}T_e = \frac{3P}{4L_M}\left((v_q^r - \omega_r \lambda_d^r)\lambda_m - \frac{4r_s}{3P}T_e\right)\boldsymbol{e}_z \quad . \tag{3.33}$$

For small T_s

$$\frac{d}{dt}T_e \approx \frac{T_e[\mathrm{k}+1] - T_e[\mathrm{k}]}{T_s} \tag{3.34}$$

which gives

$$\Delta T_e[\mathrm{k}] = \frac{3PT_s}{4L_M}\left((v_q^r[\mathrm{k}] - \omega_r \lambda_d^r[\mathrm{k}])\lambda_m - \frac{4r_s}{3P}T_e[\mathrm{k}]\right) \tag{3.35}$$

From the above expressions it can be seen how torque is affected depending on working conditions. As can be seen, the last term, $-4r_s/(3P)T_e$, always tries to counteract the torque and make it approach the origin.

Assume motor operation and positive rotational direction. Then the average v^r_q is positive, speed induced voltage, $-\omega_r \lambda^r_d$, negative, and an asymmetry becomes clear.
If torque is too low and need to be increased a positive v^r_q is chosen, but because of $-\omega_r\lambda^r_d$ is suppressed and increasing torque becomes more difficult at high velocities. On the other hand, if torque is too high, a negative v^r_q is chosen but is now boosted which make torque decreases more at high velocities.

It is always reasonable to assume $\lambda^r_d > 0$. If λ^r_d should be negative the demagnetizing flux must be greater than the flux produced by the permanent magnet which may demagnetize the magnet permanently.

3.3. System analysis

Now when all results needed for analysis purposes are obtained we can start looking at the results.

To see how the voltage selection criterion is made it is good to know how the voltage vectors influence flux and torque over a sector.
From the orientation of the λ_s-reference one can see that $v_d^{\lambda s}$ is the component controlling the flux, because $v_d^{\lambda s}$ is aligned with the flux vector. It seems reasonable to assume then that $v_q^{\lambda s}$ is responsible for the torque control.

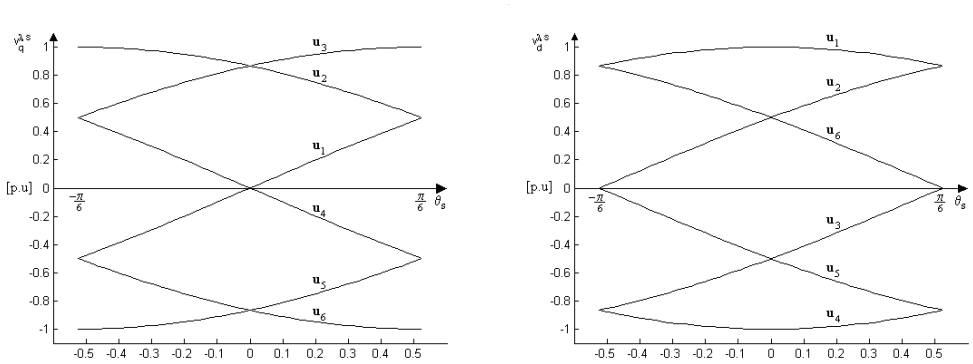

Figure 3.12, $q^{\lambda s}$ and $d^{\lambda s}$ voltage components for the six available vectors over sector 1

As can be seen there are three vectors that tend to increase the flux; u_1 u_2 and u_6, and three tending to decrease it; u_3 u_4 and u_5.
Since $v_q^{\lambda s}$ is assumed to control torque, there are two vectors; u_2 and u_3 that tend to increase it while u_5 and u_6 tend to decrease it. Both u_1 and u_4 are negative for half the sector and positive for the other half and thus, can not be chosen since the same selection criteria is used over the whole sector.

Now let's return to the basic switch table utilizing only active vectors, shown in Table 3.1.

d_λ	d_T	N = 1
-1	-1	u_5
	1	u_3
1	-1	u_6
	1	u_2

Table 3.2, Switch table for sector 1

u_5 should decrease both flux and torque. From figure 3.12 and the discussion above, u_5 is the only vector that fulfills the requirements over the whole sector. u_3 has a positive $q^{\lambda s}$ and negative $d^{\lambda s}$ component and will increase torque while decreasing flux. Similarly u_2 and u_6 are the most appropriate choices.
For the other sectors only a rotation of the vectors is needed. In sector 2 for example, u_5 is replaced by u_6, u_3 by u_4 etc.

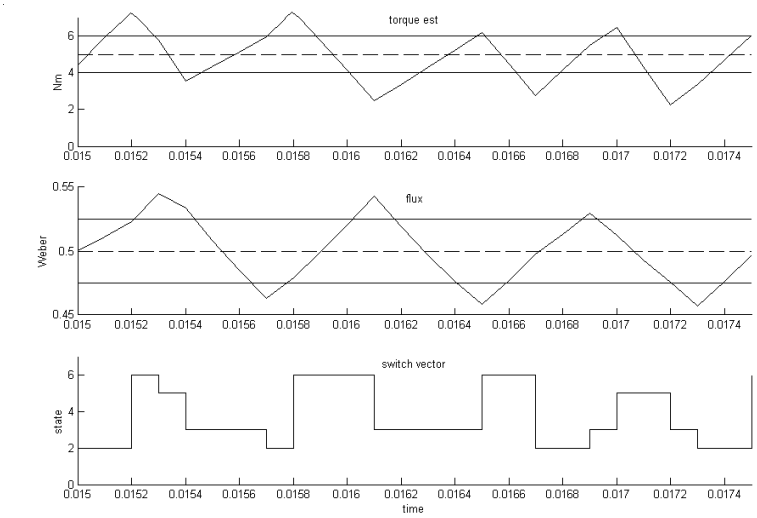

Figure 3.13, How DTC chose switch vectors depending on torque and flux

Figure 3.13 shows the DTC voltage vector selection in sector 1. The dashed lines are command values and solid lines hysteresis thresholds.

Eq. (3.35),

$$\Delta T_e[\mathrm{k}]=\frac{3PT_s}{4L_M}\left((v_q^r[\mathrm{k}]-\omega_r\lambda_d^r[\mathrm{k}])\lambda_m-\frac{4r_s}{3P}T_e[\mathrm{k}]\right) \quad . \tag{3.36}$$

Divide this equation into two contributions,

$$\Delta T_e=\Delta T_2+\Delta T_1 \quad . \tag{3.37}$$

The first contribution

$$\Delta T_1=-T_s\frac{r_s}{L_M}T_e \tag{3.38}$$

always tries to lower the torque value. The second contribution,

$$\Delta T_2=\frac{3PT_s}{4L_M}\left(v_q^r-\omega_r\lambda_d^r\right)\lambda_m \quad , \tag{3.39}$$

is the component controlled by the applied voltage vector. The voltage vector controlling torque and the flux component giving rise to the emf are both expressed in the rotor reference. From figure 3.9 and 3.11

$$v_q^r=v_q^{\lambda s}\cos(\gamma) \tag{3.40}$$

and

$$\lambda_d^r = \lambda_s \cos(\gamma) \quad . \tag{3.41}$$

Thus, when ΔT_2 is expressed in the λ_s-reference it becomes

$$\Delta T_2 = \frac{3PT_s}{4L_M}\left(v_q^{\lambda s} - \omega_r \lambda_s\right)\lambda_m \cos(\gamma) \quad . \tag{3.42}$$

The relation between applied vector and emf is maintained. The difference is that when γ grows the effect of $v_q^{\lambda s}$ on ΔT_2 is weaker.
In the extreme case, when γ = +/- 90º, $v_q^{\lambda s}$ no longer affects torque but is instead controlled by $v_d^{\lambda s}$. This happens if the demagnetizing flux, $L_M i^r_d$, exactly cancels the magnet flux. Hence, if γ becomes too big, decoupled flux and torque control is no longer possible, and the control strategy used in DTC does not work.

But because γ is normally quite small this is seldom a problem. For example the motor used in the experiments has a nominal current of 5A, a q-axis inductance of 0.043H and a PM flux of 0.49Wb. That is, when the nominal current is directed along the q^r-axis, to obtain maximum torque per ampere ratio, $\cos(\gamma) \approx 0.9$, which is close to one.

Only when the motor is hardly demagnetized, as may be the case in the flux weakening region, the difference becomes important.

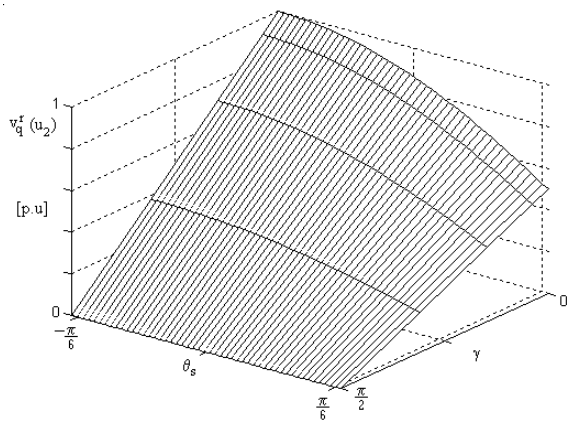

Figure 3.14, How torque producing component v^r_q depends on flux angle and γ

The above figure shows how the torque producing component, v^r_q, depends on the flux and γ when u_2 is applied and λ_s is in sector 1.

Depending on the operating conditions a given voltage vector may affect torque quite differently. When the rotor evolves an emf is induced in the stator windings. This voltage, $\omega_r\lambda_d$, has the same direction as v_q in motor operation.

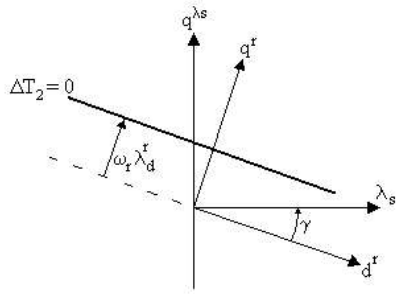

Figure 3.15, Induced emf change the effect of a voltage vector on torque

This emf makes an increase of torque value more difficult when speed is high while a decrease is more significant. Another effect is that if speed is low and torque is close to the desired value a zero vector may be applied. A zero vector "locks" the stator current at its actual value and position and hence, if rotor movement may be neglected (which is the case for short T_s and low speed), maintains torque at the same value.
For high speeds a zero vector will decrease torque because of $\omega_r \lambda_d$, as seen in the figure. This problem is dealt with in the DSVM scheme, where more voltage vectors are available.

3.4. Some problems with the basic DTC system

Torque ripple

A mayor disadvantage with the DTC control is its high torque ripple. In some applications this may not be a problem, rotor and load inertia filters the ripple, while in some applications low torque ripple is essential.
A Field Oriented Controller produce less ripple but has the drawback of being more complex and less robust than a DTC controller.

Drift in Flux Estimator

Direct Torque Control is very robust because it only uses one system parameter, stator winding resistance. This parameter, however, affects the stator flux estimation which is the heart of a DTC.
A deviance in stator resistance cause an under or over estimation of stator flux, if the estimator is implemented as an integrator, even the smallest discrepancy will eventually make the integrator drift away.
Since a DTC control system normally is implemented in discrete time and no measurement can ever be perfect, a pure integrator is prone to drift.

Stator resistance has a high influence on flux estimation, especially at low speed where resistive voltage drop is comparable with the speed voltage.
During operation stator resistance will change due to temperature changes caused by copper losses in stator windings, heating in nonlinear magnetic materials, etc. The stator resistance may change by about 1.5 – 1.7 times of its nominal value [23].
When the difference between actual resistance and the value used in flux estimation becomes sufficiently large, the control system may become unstable.
A solution to minimize this problem is to use an online resistance estimator.
If actual resistance is larger than that used in the flux estimation, an overestimation of flux will result. The flux then gives an overestimation of calculated torque.
If the resistance were not different, current had to differ from its measured value. This difference in measured and a hypothetical current can drive a PI-estimator that tracks the resistance. The integral part force estimated resistance to converge to its real value until there is no difference between the hypothetical and measured current.

The problem with integrator drift may be solved by using n cascaded low-pass filters.
If n 1:st order filters are connected in series the total phase shift and gain become

$$\phi_T = n \arctan(\tau \omega) \tag{3.43}$$

$$K_T = (1+(\tau \omega)^2)^{\frac{-n}{2}} \quad . \tag{3.44}$$

For the cascaded filters to work as an integrator their total phase shift should be 90º and compensation gain must be used so that the overall gain is 1/ω. From these conditions one calculates the time constant and compensating gain,

$$\tau = \frac{1}{\omega} \tan\left(\frac{\pi}{2n}\right) \tag{3.45}$$

$$G = \frac{1}{\omega}(1+(\tau \omega)^2)^{\frac{n}{2}} \quad . \tag{3.46}$$

The LPFs cannot operate as an integrator for zero frequency because time constant and gain becomes infinite. The method has the drawback of requiring more computations but does not drift and therefore significantly improves drive performance.

Summary

Chapter 3 begun with an explanation of the DTC scheme's different blocks. Section 3.2 express the flux vector in different reference frames and derive an equation for the torque. From these expressions one can see how the DTC voltage vector selection strategy is made.

Different working conditions influence how a given voltage vector affect flux and torque. Torque ripple will be symmetrical around its reference value at low speed while at higher speeds the emf voltage tries to decrease torque and eventually makes it impossible to increase. For high velocities the rotor flux must be weakened in order for the machine to be able to produce torque.

An advantage of DTC is the possibility of not requiring a position decoder during operation. The flux vector estimator, which is the heart of a DTC, only needs to know the stator winding resistance and initial rotor position. If care is not taken when operating a DTC system sensor-less the drive system will be prone to instability. On-line estimation of stator resistance and the use of cascaded low-pass filters to perform the required integration are two viable solutions to minimize the problems and enhance drive performance.

Chapter 4 Discrete Space Vector Modulation

This chapter presents an improved DTC system. The system is called Discrete Space Vector Modulation – DTC [11] or just DSVM. The system addresses the problem with torque ripple in the basic DTC system.

The name DSVM stems from the fact that the system divides each sample period in three equal time intervals to produce a kind of Space Vector Modulation, and hence, being able to produce more precise voltage vectors. The system still use predefined switch tables so the simplicity of the basic DTC scheme is maintained.

4.1 Introduction to the DSVM – DTC system

Section 3.1 presented the different blocks of the DTC system. Most of the blocks found in the DSVM system are the same as those found in the DTC system and only the differences will be discussed.

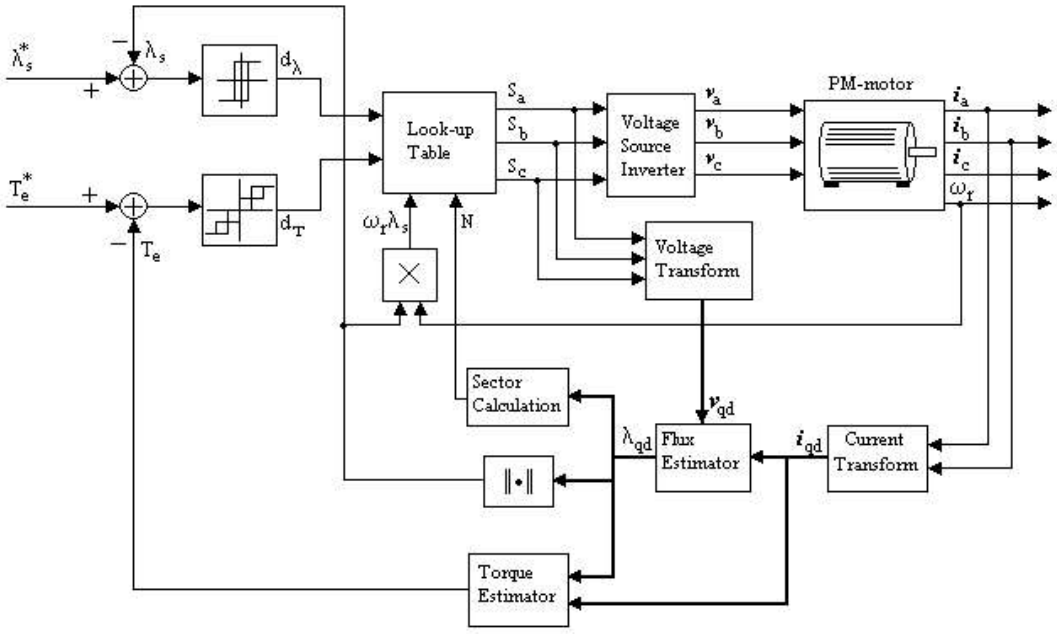

Figure 4.1, DSVM system block diagram

Speed voltage

In section 3.2 was mentioned an asymmetry in torque behavior because of speed induced voltage. The DSVM calculates this voltage and use it to choose an appropriate voltage

vector. The operating range from zero speed up to where induced voltage equals the applied voltage vectors is divided into three region; Low, Medium and High.

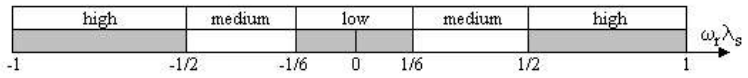

Figure 4.2, Speed voltage regions, [p.u]

The voltage induced is

$$\omega_r \begin{bmatrix} \lambda_d \\ -\lambda_q \end{bmatrix} \quad .$$

But only its value is used, so calculated voltage is

$$v_s = \omega_r \lambda_s \quad , \tag{4.1}$$

which is then compared to the regions.

Sector calculation

The DSVM use twelve sectors instead of six; all of the six sectors in DTC are divided in half. The finer division of sectors is used in the high-speed region. At medium and low speed range only six sectors are used.

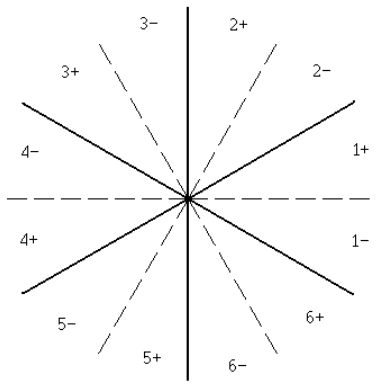

Figure 4.3, DSVM sectors

Torque hysteresis

The DSVM can produce more voltage vectors which if properly applied produce less ripple. To achieve this, the torque hysteresis has 5 levels instead of two.

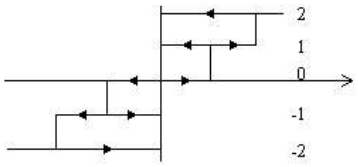

Figure 4.4, 5-level hysteresis comparator

If torque error is small hysteresis is in state 0. In this case a voltage vector is chosen trying to maintain torque at its actual level. If hysteresis is in state +/– 1, a vector just as big as to push torque into the small region is chosen. When hysteresis is in state +/– 2, a vector compensating for the error as fast as possible is chosen, i.e. the same vectors used in the classical DTC.

Look-up Table

The look-up table in this case has four input variables; flux and torque hysteresis state, sector number and speed voltage. Since the system chose voltage vectors depending on the emf, each speed region uses different switch tables. When the system operates in the high speed region two switch tables for each sector are used. Because the emf introduces an asymmetry, the switch tables also become asymmetric. Hence, different tables must be used for positive and negative rotational directions.

Voltage Source Inverter

In DSVM each sample period is divided into three equal time intervals. In each time interval an active vector or a zero vector is applied. The inverter must therefore work at three times the sample frequency or use pulse width modulation to generate a vector.

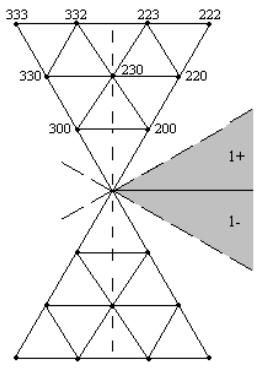

Figure 4.5, space vectors for sector 1

For example, the vector 223 is synthesized by applying u_2 the first two intervals and then u_3. If this vector instead is expressed by duty cycles it would be,

vector	duty cycle		
223	A	B	C
	0.67	1	0

This is how the inverter operated during the experiments.

4.2 Space vector selection

In chapter 3 the problems with torque ripple and the asymmetric torque behavior at high velocities were discussed. In this section will be discussed how the higher number of available voltage vectors can be utilized to reduce these problems.

When speed increase the induced emf, v_s, also increase. The voltage vector v_s leads λ_s by 90º and lies along the $q^{\lambda s}$-axis. The resultant vector that affects torque is the $v_q^{\lambda s}$ component of the applied VSI vector minus v_s. Therefore, the voltage selection criteria should use v_s as a reference; if $v_q^{\lambda s} \approx v_s$ torque is kept at the same level, $v_q^{\lambda s} > v_s$ increase torque and $v_q^{\lambda s} < v_s$ decrease it.

Low-speed region

When v_s is in the low-speed region, v_s is close to zero. The switch vectors are selected symmetrically around zero, which also connects the gap between positive and negative speed switch tables.
If estimated torque is close to its reference value and torque hysteresis is in state zero, the zero vector is chosen. If torque hysteresis is in state +1 or -1, a moderate increase or decrease, respectively, is wanted. Selection is made between u_{200}, u_{300}, u_{500} and u_{600}. u_{200} and u_{600} is the choice if flux is to be increased while u_{300} and u_{500} decrease flux. When the difference is big between estimated and reference torque, i.e. d_T = +/-2, DSVM chooses switch vectors as the DTC. Here vectors u_{222}, u_{333}, u_{555}, and u_{666} are selected in order to compensate for the deviation as fast as possible.

	d_T					
		-2	-1	0	1	2
d_λ	-1	555	500	000	300	333
	1	666	600	000	200	222

Table 4.1, Switch table for positive low-speed region, sector 1

Medium-speed region

In the medium-speed region, $v_N/6 < |v_s| < v_N/2$, the emf voltage starts to introduce an asymmetry of the switch vectors on torque behavior. For positive v_s and $d_T = 0$, DSVM chose between u_{200} and u_{300}, since these vectors makes $v_q^{\lambda s}$ approximately equal to v_s and hence maintains torque at its actual level. u_{200} is the choice if flux should be increased and u_{300} if decreased. For $d_T = -1$ a moderate torque decrease is wanted. Now the closest vector decreasing torque is u_{000}, and since this is the only vector at this level it is chosen weather flux is lower or higher than its reference value. For $d_T = +1$, u_{220} is selected when flux should be raised and u_{330} when lowered. As in the low speed region, DSVM operates as the DTC when $d_T = +/- 2$.

	d_T					
		-2	-1	0	1	2
d_λ	-1	555	000	300	330	333
	1	666	000	200	220	222

Table 4.2, Switch table for positive medium-speed region, sector 1

High-speed region

In the high-speed region, $|v_s| > v_N/2$. To make use of all vectors available each sector is divided in half.
Assume λ_s is in sector 1- . Then if torque is to be kept at the same level, vectors u_{220} and u_{230} are selected depending on the flux comparator. For $d_T = -1$, the nearest lower $v_q^{\lambda s}$ voltage is obtained by choosing u_{200} or u_{300}. For $d_T = +1$, u_{222} and u_{223} will increase flux while u_{332} and u_{333} will decrease flux. To make full use of all switch vectors and to keep flux ripple at a low level, u_{222} and u_{332} are chosen for λ_s lying in sector 1-. When λ_s is in sector 1+, u_{230} and u_{330} is the choice for $d_T = 0$, while u_{223} and u_{333} are chosen for $d_T = +1$. In the high speed region as in the low and medium, the maximal vectors available are selected for $d_T = +/- 2$.

	d_T					
		-2	-1	0	1	2
d_λ	-1	555	300	230	332	333
	1	666	200	220	222	222

Table 4.3, Switch table for positive high-speed region, sector 1-

		d_T				
		-2	-1	0	1	2
d_λ	-1	555	300	330	333	333
	1	666	200	230	223	222

Table 4.4, Switch table for positive high-speed region, sector 1+

Summary

The DSVM system divides each sample period in three equal time intervals to produce a kind of Space Vector Modulation. The system calculates the emf voltage which is used in the voltage selection procedure. If torque is close to its reference value a voltage space vector lying approximately on the emf voltage line is chosen. The space vectors next to the emf voltage levels are used for small torque corrections. For large torque errors DSVM operates as the basic DTC system. Torque ripple is reduced to approximately one third with respect to the basic DTC control. The system maintains a good dynamic torque response, which is characteristic for DTC, while still having a relatively low complexity; DSVM select a voltage space vector from predefined switch tables.
A comparison with the basic DTC can be seen in the next chapter where results from simulations and experiment are presented.

Chapter 5 Simulation and experimental results

In chapter 3 and 4 the DTC and DSVM systems were explained in detail. Here simulation and experimental results of the two systems are presented.

Simulation models are programmed in Matlab/Simulink, operating at a sample frequency of 10 kHz. Experimental arrangement consist of a dSPACE DS1103 board, connected to a Danfoss VLT5003 inverter. The PM motor is a Siemens 1FT6062-6AC7. To control the breaking torque another Siemens 1FT6084 motor is used connected to a Siemens SIMOVERT MC inverter which is controlled by the dSPACE environment.
The experiments were executed with a sample frequency of 20 kHz. Increased ripple, measure noise and conservative protections would otherwise obscure the interesting parts of the experiments.

Simulation results

Direct Torque Control shows a good dynamic torque response when compared with other control methods. However, the large torque ripple in steady-state operation is one of its major drawbacks. The improved DTC system, DSVM, can produce more voltage space vectors than the basic DTC. The larger number of space vectors are used to decrease torque ripple in steady-state operation. Figure 5.1 and 5.2 shows how the two systems behave in steady-state with the motor operating at $\omega_m = 50$ rad/s, approximately 500 rpm.

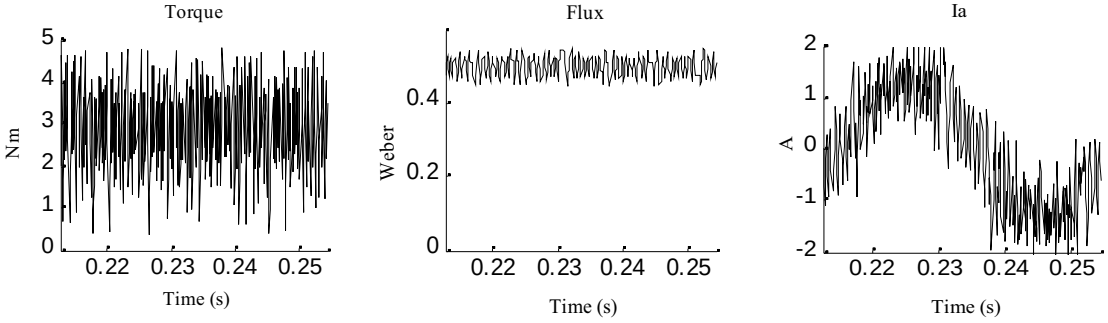

Figure 5.1, DTC steady-state behavior

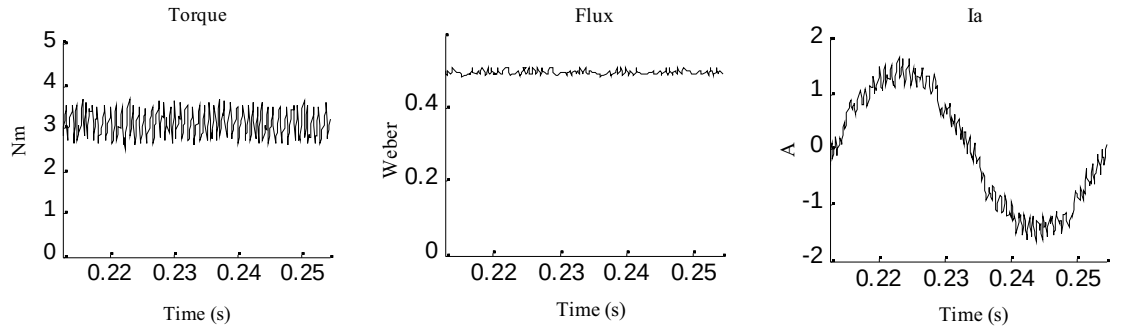

Figure 5.2, DSVM steady-state behavior

DSVM has a significantly lower ripple level both in torque, flux and stator current. A lower current ripple is also advantageous because the machine will have less EMI noise.

Figure 5.3 and 5.4 shows dynamic torque response at standstill. DSVM has as good dynamic response as the DTC. During simulations a load with the same torque value but opposite direction were applied on the motor shaft.

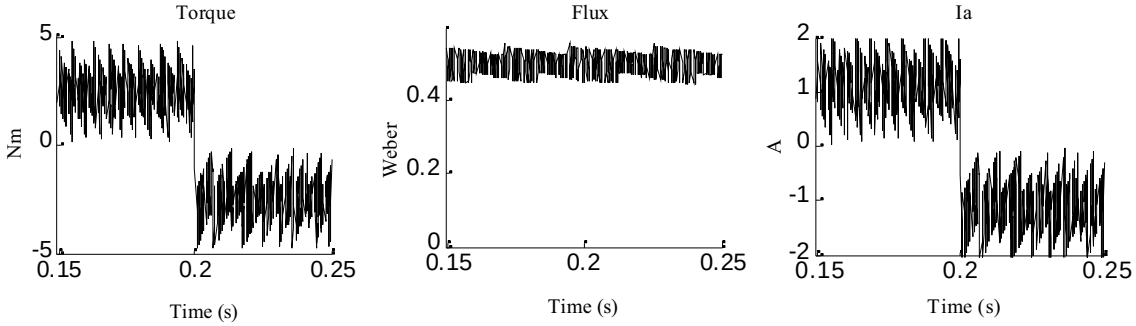

Figure 5.3, DTC dynamic response at standstill

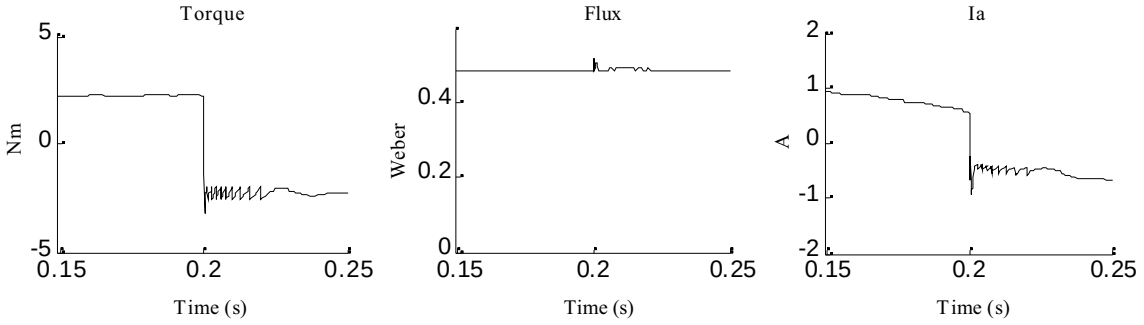

Figure 5.4, DSVM dynamic response at standstill

Reference torque changes instantly from 2.5 Nm to -2.5 Nm. The stator current i_a is slightly changing for the DSVM because the rotor is moving slowly due to a small difference between motor and load torque. The sum of the three stator currents would be

a slowly moving vector with constant amplitude.

Experimental results

Both systems have been tested experimentally in order to verify the improvements of the proposed method. Steady-state and dynamic response results were obtained under the same conditions as in simulations with the exception of a higher sample frequency.

Figure 5.5 and 5.6 shows steady-state behavior for the DTC and DSVM, respectively. The motor operates at ω_m = 50 rad/s, approximately 500 rpm. The relative decrease in ripple levels in the DSVM is similar to simulations.

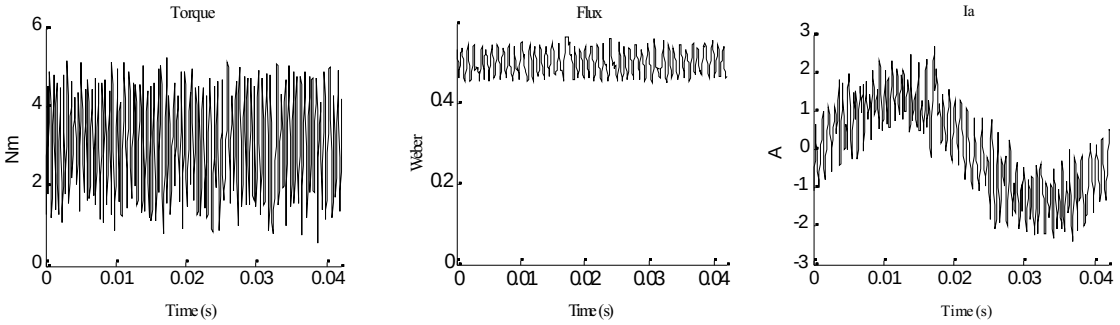

Figure 5.5, DTC steady-state behavior

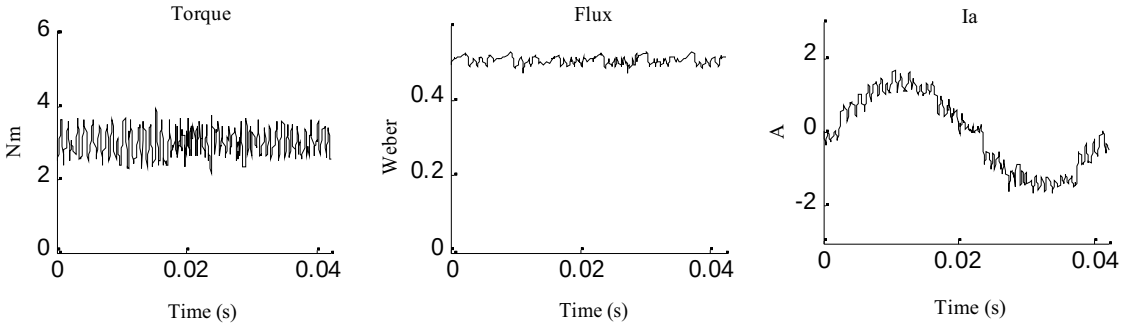

Figure 5.6, DSVM steady-state behavior

Dynamic response measurements were taken with the rotor at approx. standstill, where the load was a motor giving the same torque but in the opposite direction. Torque is greatly reduced with the DSVM scheme. Ripple reduction complies well with eq. (3.35) predicting a torque ripple reduction to 1/3 compared with the basic DTC scheme, since each sample interval is divided into three equal parts.

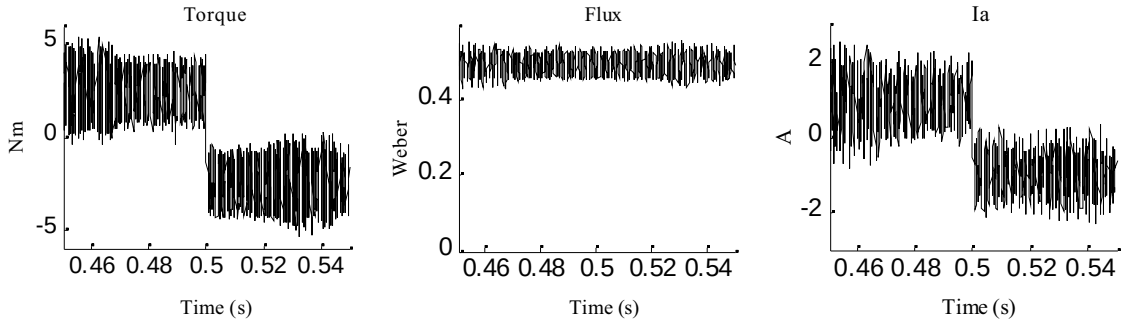

Figure 5.7, DTC dynamic response at standstill

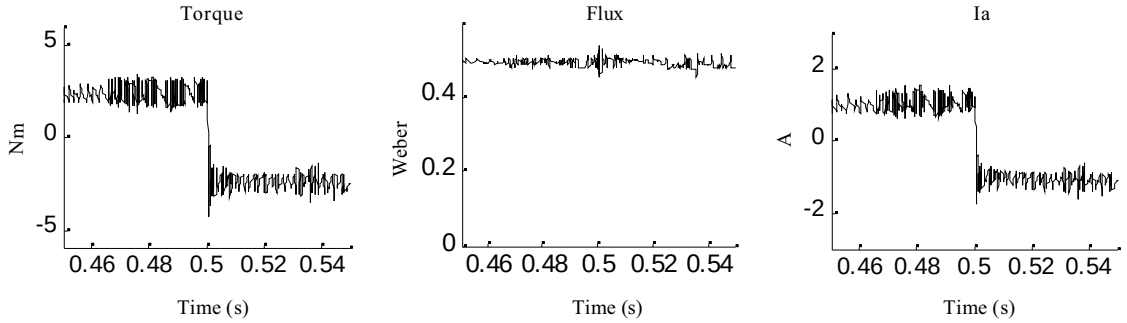

Figure 5.8, DSVM dynamic response at standstill

Figure 5.9 shows a staircase response. The visible spikes in the DSVM plot are because the dSPACE platform now and then loses itself. These figures show the transition from 2.5 to 5 Nm is almost as fast as from 0 to 2.5 Nm. This is good because it is harder to increase torque from an already high level.

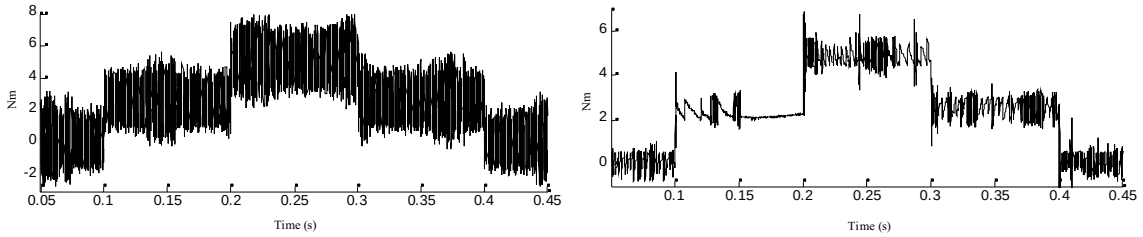

Figure 5.9, DTC and DSVM staircase torque response

Summary

The above simulation and experimental results shows the DSVM system having less torque ripple while it maintains as good torque response as the basic DTC. It still use switch tables to select a voltage vector so complexity is only slightly increased. In fact, it is possible to run the DSVM system at half the sample frequency compared to the DTC

and still obtain equal or lower ripple levels. DSVM would in this case require less of the processor.

Chapter 6 Conclusion

This work has dealt with the Direct Torque Control and one of its improved variants proposed in the research literature. DTC was introduced in the 1980´s by I. Takahashi, T. Noguchi and M. Depenbrock (DSC) and was a novel control technique for Induction Motor vector control. Vector control was introduced in 1972 by F. Blaschke which was the technique since known as Field Oriented Control.
In vector control both amplitude and position of the field flux is known, so the controller can control the armature flux amplitude and angle relative the field flux. In a DC motor the field flux, which in this case is the stator flux, and the armature flux (rotor) are held orthogonal mechanically by the commutator. When the fields are orthogonal, armature flux does not affect the field flux and the motor torque responds immediately to a change in armature flux or equivalently, armature current. In an AC motor the field flux (which now is in the rotor) rotates, but in a FOC the controller rotates the armature (stator) flux so that armature and field flux are kept orthogonal, and hence, the motor-controller system behaves as a DC motor system.
The principle behind Direct Torque Control is quite the same, with the difference the control action is tabulated instead of being calculated online. DTC being more crude has the advantage of not having to compute applied current/voltage vectors, which significantly lowers the computational burden. This allows for a pretty simple, and cheap, processor to perform the task. Another feature of not computing the CSI or VSI vectors online is that fewer motor parameters are involved in the control, which improves robustness.
The decreased performance of DTC drives in terms of torque, flux and current ripple, with respect to FOC, is partly compensated for by its simplicity since this allows for higher sample frequencies. The problem is that the inverter sets an upper limit for its switching frequency.
Since the introduction of DTC a lot of research has been done to improve performance of DTC drives while maintaining the good properties, such as

- low complexity
- good dynamic response
- high robustness.

In this work one of the many improved DTC systems proposed is presented. Simulation and experimental results confirms its validity.
The new DTC system called Discrete Space Vector Modulation – DTC or just DSVM, use a kind of space vector modulation to produce more voltage vectors than are available with the classical DTC. DSVM use different look-up tables depending on the value of the emf voltage induced in the stator windings.
Both the classical and improved DTC systems are simulated using Simulink and then ran on a dSPACE platform to evaluate real life behavior from the experiments. The systems show a higher ripple level for torque, flux and stator currents in the experiments than in the simulations. Though, the relative decrease in ripple levels of the DSVM system

compared to the DTC system are equal both in experiments and simulations.

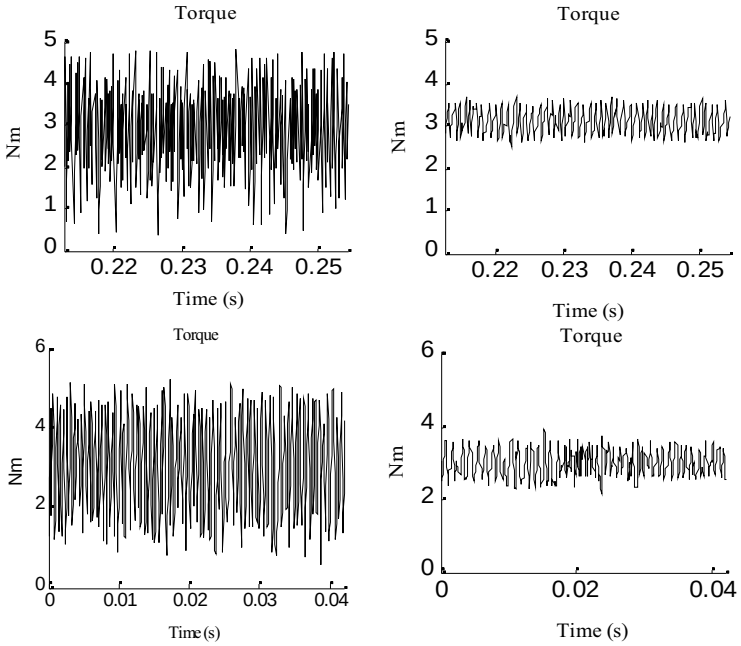

Figure 6.1, Above simulation results; left DTC, right DSVM.
Below experimental results; left DTC, right DSVM.

The DSVM is a compromise between performance and low complexity because the use of look-up tables. While a large number of voltage vectors would improve performance in terms of low ripple, they would require large and complex look-up tables. The benefits of the proposed method is that while complexity is still low, ripple levels are decreased and the good dynamic response is maintained, which the experimental results in figure 6.2 shows.

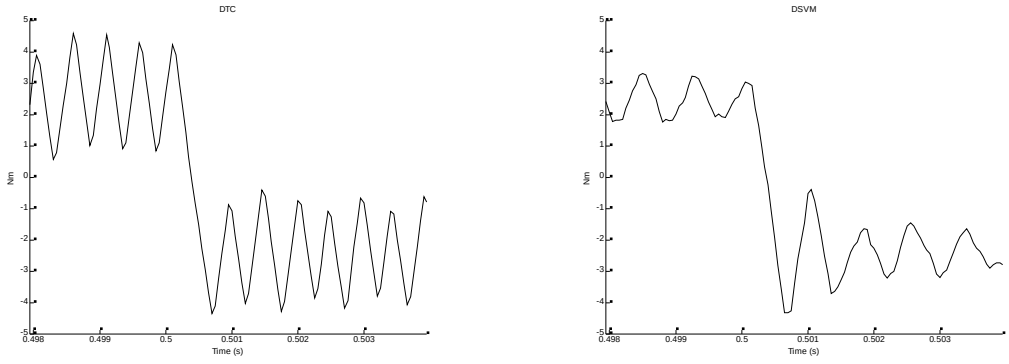

Figure 6.2, Dynamic response DTC and DSVM

There are other methods performing better than the one presented, but at the expense of higher complexity and computational burden.

With the introduction of Field Oriented Control, AC motors have in many applications replaced DC motors where good torque control and fast dynamic response is required. The AC motor being more reliable, requiring less maintenance and being the preferred choice in hazardous environments, e.g. if explosive gas is present, where sparks from the commutator in a DC motor is a problem.
With the commercialization of DTC, the first commercial products introduced by ABB, the technique is now being employed where before FOC drives were used.

References

1. Modern Power Electronics and AC Drives
Bimal K.Bose
2002 Prentice Hall, ISBN 0-13-016743-6

2. Dynamic simulation of Electric Machinery using Matlab/Simulink
Chee-Mun Ong
1998 Prentice Hall, ISBN 0-13-723785-5

3. Vector Control and Dynamics of AC Drives
D.W. Novotny, T.A. Lipo
1996 Oxford University Press, ISBN 0-19-856439-2

4. Analysis of Electric Machinery and Drive Systems, Second Edition
Paul C. Krause, Oleg Wasynczuk, Scott D. Sudhoff
2002 IEEE Press, Wiley Interscience, ISBN 0-471-14326-X

5. Electric Machinery, fourth edition
A.E. Fitzgerald, Charles Kingsley Jr., Stephen D. Umans
1983 McGraw-Hill, ISBN 0-07-021145-0

6. Advanced Control System Design
Bernard Friedland
1996 Prentice Hall, ISBN 0-13-010653-4

7. Feedback Control of Dynamic Systems, third edition
Gene F. Franklin, J. David Powell, Abbas Emami-Naeini
1994 Addison-Wesley, ISBN 0-201-52747-2

8. Electromechanical Systems, Electric Machines and Applied Mechatronics
Sergey E. Lyshevski
CRC Press 2000, ISBN 0-8493-2275-8

9. Field and Wave Electromagnetics, Second Edition
David K. Cheng
1989 Addison – Wesley, ISBN 0-201-52820-7

10. Elementary Linear Algebra, 7th Edition
Howard Anton, Chris Rorres
1994 Wiley, ISBN 0-471-58741-9

11. Improvement of Direct Torque Control by Using a Discrete SVM Technique
Domenico Casadei, Giovanni Serra, Angelo Tani
IEEE 1998

12. Torque dynamic behavior of Induction machine DTC in 4 quadrant operation
I. El Hassan, X. Roboam, B. de Fornel, E.V. Westerholt
IEEE 1997

13. Analytical Formulation of the Direct Control of Induction Motor Drives
M. Bertoluzzo, G. Buja, R. Menis
1999 IEEE

14. Direct Torque Control of Permanent Magnet Synchronous Motor (PMSM) Using Space Vector Modulation (DTC-SVM) – Simulation and Experimental Results
Dariusz Swierczynski, Mariam P. Kazmierkowski
2002 IEEE

15. A New Direct Torque Control Strategy for Flux and Torque Ripple Reduction for Induction Motors Drive – A Matlab/Simulink Model
Lixin Tang, M.F. Rahman
2001 IEEE

16. A Direct Torque Controller for Permanent Magnet Synchronous motor drives.
Zheng, M.F. Rhaman, W.Y. Hu, K.W. Lim.
IEEE transactions on energy conversion, Vol. 14, No. 3, September 1999.

17. Study on the Direct Torque Control of Permanent Magnet Synchronous Motor Drives.
Sun Dan, Fang Weizhong, He Yikang.
Electrical Machines and Systems, IEEE 2001

18. Implementation Strategies for Concurrent Flux Weakening and Torque Control of the PM synchronous Motor.
Ramin Monajemy, Ramu Krishnan.
IEEE, Industry Applications Conference, 1995.

19. FOC and DTC: two viable schemes for induction motors torque control.
Domenico Casadei, Fransesco Profumo, Giovanni Serra, Angelo Tani.
IEEE Transactions on Power Electronics, 2001.

20. Direct torque control of induction motors: stability analysis and performance improvement.
Romeo Ortega, Nikita Barabanov, Gerardo Escobar Valderrama.
IEEE Transactions on Automatic Control, Vol. 46, No. 8, 2001.

21. Direct stator flux linkage control technique for a permanent magnet synchronous machine.
A.M. Llor, J.M. Rétif, X. Lin-Shi, S. Arnalte
IEEE 2003

22. Direct Torque Control of PWM Inverter-Fed AC Motors – A Survey
Giuseppe S. Buja, Marian P. Kazmierkowski
IEEE Trans. On Industrial Electronics, Vol. 51, No. 4, August 2004

23. Problems Associated With the Direct Torque Control of an Interior Permanent-Magnet Synchronous Motor Drive and Their Remedies
Muhammed Fazlur Rahman, Enamul Haque, Lixin Tang, Limin Zhong
IEEE Trans. On Industrial Electronics, Vol. 51, No. 4, August 2004

24. A Space Vector Modulation Direct Torque Control for Permanent Magnet Synchronous Motor Drive Systems
D. Sun, J.G. Zhu, Y.K. He
Power Electronics and Drive Systems, IEEE 2003

25. Study of Direct Torque Control (DTC) System of Permanent Magnet Synchronous Motor Based on DSP
Dai Wenjin, Li Huiling
Electrical Machines and Systems, IEEE 2001

Appendix

I. Motor parameters

Siemens 1FT6062-6AC7			
Quantity	Symbol	Unit	Value
Nominal rpm	n_N	1/min	2000
Pole number	P		6
Nominal torque	T_N	Nm	5.2
Nominal current	I_N	A	2.6
Inertia	J	$kg \cdot m^2$	$8.5 \cdot 10^{-4}$
Stator resistance	r_s	Ω	5.8
Magnetizing inductance	L_M	mH	43
Rotor flux	λ_m	Wb	0.49

Table I.1, Motor parameters